JGR Biogeosciences

RESEARCH ARTICLE
10.1029/2022JG007096

Nonlinear Growth and Physiological Responses of White Spruce at North American Arctic Treeline

Mathieu Lévesque[1,2], Laia Andreu-Hayles[2,3,4], Rosanne D'Arrigo[2], Rose Oelkers[2], and Brendan M. Buckley[2]

[1]Silviculture Group, Institute of Terrestrial Ecosystems, ETH Zurich, Zurich, Switzerland, [2]Tree-Ring Laboratory, Lamont-Doherty Earth Observatory of Columbia University, Palisades, NY, USA, [3]CREAF, Barcelona, Spain, [4]ICREA, Barcelona, Spain

Key Points:

- Complex growth and physiological responses of white spruce trees to changes in temperature and sea ice extent inferred from stable isotopes
- White spruce radial growth at Arctic latitudinal treeline decreased at an interior site and increased at a site closer to the Arctic Ocean
- White spruce shifted from a passive to an active water-use efficiency response to rising CO_2 concentration over the 20th century

Supporting Information:

Supporting Information may be found in the online version of this article.

Correspondence to:

M. Lévesque and L. Andreu-Hayles, mathieu.levesque@usys.ethz.ch; lah@ldeo.columbia.edu

Citation:

Lévesque, M., Andreu-Hayles, L., D'Arrigo, R., Oelkers, R., & Buckley, B. M. (2023). Nonlinear growth and physiological responses of white spruce at North American Arctic treeline. *Journal of Geophysical Research: Biogeosciences*, *128*, e2022JG007096. https://doi.org/10.1029/2022JG007096

Received 13 JUL 2022
Accepted 31 MAR 2023

Author Contributions:

Conceptualization: Mathieu Lévesque, Laia Andreu-Hayles
Data curation: Laia Andreu-Hayles, Rosanne D'Arrigo, Rose Oelkers, Brendan M. Buckley
Formal analysis: Mathieu Lévesque
Funding acquisition: Laia Andreu-Hayles, Rosanne D'Arrigo
Investigation: Mathieu Lévesque, Laia Andreu-Hayles, Rosanne D'Arrigo, Rose Oelkers

Abstract Much is still unknown about the growth and physiological responses of trees to global change at the northern treeline. We combined tree-ring width data with century-long stable carbon and oxygen isotope records to investigate growth and physiological responses of white spruce at two treeline sites in the Canadian Arctic to concurrent increases in temperature, atmospheric CO_2 concentration (c_a), and decline in sea ice extent over the past century. The tree-ring records were assessed during three periods with contrasting climatic conditions: (a) the early 20th century warming, (b) the 1940–1970 cooling period, and (c) the anthropogenic late 20th century warming period. We found opposing growth trends between the two sites, but similar carbon isotope discrimination ($\Delta^{13}C$) and intrinsic water-use efficiency ($_i$WUE) trajectories. While tree growth (defined as basal area increment) increased at the site nearer to the Arctic Ocean during the 20th century following the rise in temperature and sea ice loss, growth declined after 1950 at the more interior site. At both sites, $\Delta^{13}C$ slightly increased over these periods. However, trees showed a nonlinear response to increased c_a, shifting after 1970 from a passive stomatal response (i.e., no changes in $_i$WUE) to an active response (i.e., a moderate ~12% increase in $_i$WUE). Further, our isotope-based findings do not support the idea that temperature-induced drought stress caused the divergent growth trends at our treeline sites. This study thus highlights nonlinear and complex physiological and growth adjustments to concomitant changes in temperature, sea ice extent, and c_a over the last century at the northern treeline.

Plain Language Summary In the last decades, Arctic ecosystems have experienced unprecedented warmer temperatures, higher atmospheric carbon dioxide concentrations, and a decline in sea ice extent. However, it is still unknown how these changes in environmental factors have impacted tree populations at their northern distribution limits. Here, we examine how the growth and water-use efficiency of white spruce trees have changed over the last century in response to warmer temperatures, higher carbon dioxide concentrations, and sea ice decline at two treeline sites in the Canadian Arctic. We found that tree growth increased at the site nearer to the Arctic Ocean during the 20th century following the rise in temperature and sea ice loss, while growth declined after 1950 at the more interior site. At both sites, the water-use efficiency of trees was stable until 1970. Following the rapid temperature and carbon dioxide increase since the 1970s, trees have become more efficient in using water. The contrasting growth trends found at our study sites highlight complex growth and physiological adjustments of white spruce trees to rapid and simultaneous changes in temperature, sea ice extent, and carbon dioxide concentrations in the Arctic.

1. Introduction

The boreal forest biome covers a quarter of the Earth's terrestrial surface and plays a critical role in the global carbon and water cycles. Approximately one third of the globe's terrestrial carbon stock is stored in boreal forests (Bradshaw & Warkentin, 2015; Pan et al., 2011), where the growth of trees is responsible for most of the carbon sink activity in the Arctic (McGuire et al., 2009). These high-latitude forests are ecologically sensitive regions and can show amplified response to the strong warming observed in the Arctic (Chapin et al., 2005; Seddon et al., 2016). In the last few decades, global warming and related changes in surface hydrology and energy budgets (Chapin et al., 2010, 2005) have led to substantial changes in forest productivity and structure (Beck et al., 2011). These changes have been quite pronounced at the Arctic latitudinal treeline where unprecedented changes in vegetation composition and growth have occurred (Pearson et al., 2013).

Methodology: Mathieu Lévesque, Laia Andreu-Hayles
Project Administration: Laia Andreu-Hayles
Visualization: Mathieu Lévesque
Writing – original draft: Mathieu Lévesque
Writing – review & editing: Mathieu Lévesque, Laia Andreu-Hayles, Rosanne D'Arrigo, Rose Oelkers, Brendan M. Buckley

Shifts in temperature and moisture availability can directly impact tree physiology and forest productivity. In particular, warming may directly promote tree growth in regions where carbon assimilation and xylogenesis are limited by cold temperatures such as latitudinal treeline forests (Körner, 2012; Rossi et al., 2013). However, increasing evaporative demand due to rising air temperatures can cause drought-induced stomatal closure (Grossiord et al., 2020) and lead to growth reduction even in high-latitude forests (Barber et al., 2000; D'Arrigo et al., 2008; Jacoby & D'Arrigo, 1995; Wilmking et al., 2004). Further, rapid warming in the Arctic triggers feedbacks—for example, permafrost thaw, which in turn impacts soil hydrology and stand-level biochemistry, thus influencing moisture availability and growth of trees (Chapin et al., 2010). In parallel to the rapid climatic warming in the Arctic, sea ice extent has drastically declined in the last few decades (Brennan et al., 2020; Cai et al., 2021). Reductions in sea ice extent, in turn, alter surface albedo and ocean-atmosphere moisture flux (Kopec et al., 2016), hence feeding back into the Arctic regions and greater global climate system (Vihma, 2014). As a result, warming-amplified sea ice decline can indirectly alter terrestrial ecological dynamics in the Arctic (Buchwal et al., 2020; Post et al., 2013).

In response to these ongoing environmental changes in the Arctic, vegetation productivity has rapidly changed, but not uniformly, as there are microsite and local to regional differences (Berner et al., 2020). For example, warming and the concomitant reduction in sea ice extent have triggered heterogenous growth response of shrubs over the Arctic tundra (Buchwal et al., 2020) and trees in boreal forests (Girardin et al., 2014). Although warming has enhanced shrub growth and expansion in some regions of the Arctic (e.g., in Alaska; Andreu-Hayles et al., 2020), contrasting growth response to warming and changes in moisture availability have also been reported for the high-latitude (>65°N) boreal forest biome of North America. While some studies indicate widespread decreases in forest productivity and increased mortality (Barber et al., 2000; Girardin et al., 2016; Lloyd & Bunn, 2007) due to temperature-induced water stress (Walker et al., 2015), growth trends overall have been variable and nonlinear. At some sites, trees have shown positive growth responses to warming, while at other sites negative growth response or no trend were reported (Andreu-Hayles et al., 2011a; Lloyd & Fastie, 2002; Sullivan et al., 2017; Wilmking et al., 2004). The reasons for the observed differences between sites and tree-ring parameters (e.g., ring width vs. wood density) in temperature and moisture sensitivity (D'Arrigo et al., 2009) are not yet well understood because complex environmental factors interact in time and space.

Rising c_a may theoretically counteract warming-induced tree growth decline or even enhance growth and forest productivity by stimulating leaf-level photosynthesis and water-use efficiency—the so called CO_2 fertilization effect (Cernusak et al., 2019) —in regions where temperature, water, and nutrients are not limiting tree physiology (Norby et al., 2010; Peñuelas et al., 2011). Therefore, this stimulation of photosynthesis does not necessarily translate into enhanced radial growth (e.g., Andreu-Hayles et al., 2011b; Lévesque et al., 2014). Distinct coherency between plant processes related to carbon sources and sinks depending on environmental conditions has been reported and discussed (Andreu-Hayles et al., 2022 and references therein), and new evidence of decoupling between carbon assimilation and sinks has been found in a global study that compared flux tower and tree-ring width measurements (Cabon et al., 2022).

So far, there is little scientific consensus regarding how forests may respond to the concurrent increases in global temperatures and c_a (Cernusak et al., 2019; Lavergne et al., 2019; Peñuelas et al., 2011) especially at the Arctic treeline, where century-long physiological acclimations of treeline trees are still largely unknown. Therefore, understanding growth and physiological responses of treeline trees to the concomitant changes in temperature, sea ice extent, and c_a over the last century is a high priority. For this purpose, analysis of century-long tree-ring data (width, stable carbon and oxygen isotopic ratios) could yield novel and long-term information on forest response to environmental changes that occurred in the Arctic during the last century.

Here, we use tree-ring width and tree-ring stable carbon ($\delta^{13}C$) and oxygen ($\delta^{18}O$) isotope chronologies to assess the growth and physiological changes of white spruce trees to global warming, sea ice decline, and rising c_a over the 20th century at two remote Arctic treeline sites (one near the Arctic Ocean; the other interior; Figure 1) where century-long responses of treeline trees are still unknown, in part due to the scarcity of isotopic and other data. Our analysis covered three distinct periods with contrasting temperatures: the early 20th century warming (1900–1940), which was widespread at high latitudes in the Northern Hemisphere (Hegerl et al., 2018; Yamanouchi, 2011); the 1941–1970 period characterized by no warming/cooling; and the late 20th century warming (Kaufman et al., 2009). Specifically, we addressed the following questions: (a) How did growth and gas exchange of latitudinal treeline trees change in the 20th century; (b) Which climate variables were more important

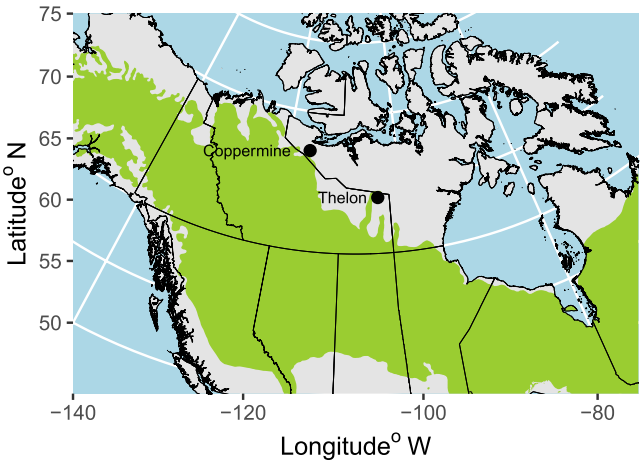

Figure 1. Location of the study sites and distribution of white spruce (green shading) in this region of North America. Species distribution data are from Little (1971) and are available online (https://databasin.org/datasets/0dd88c1ae391403698fbc9d457154bdc).

for tree growth and gas exchange for the three study periods with contrasting temperatures trends?; and (c) What were the growth and physiological responses of Arctic treeline trees to simultaneous changes in temperature and sea ice extent over the last century?

2. Materials and Methods

2.1. Study Area

We developed novel annually resolved isotopic ($\delta^{13}C$, $\delta^{18}O$) chronologies from white spruce (*Picea glauca* [Moench] Voss) samples from trees collected along the Coppermine River (67°23'N/115°92'W, 210 m a.s.l.) and Thelon River (64°03'N/103°87'W, 160 m a.s.l.) located in Nunavut and the Northwest Territories, Canada, respectively (Figure 1). The trees sampled at Coppermine were located about 75 km from the Arctic Ocean whereas those at Thelon were situated ca. 400 km from the Arctic Ocean and ca. 600 km from Hudson Bay. These two latitudinal treeline tree-ring sites have been previously used by D'Arrigo et al. (2009) for inferring past climate variability in North American Arctic, but not for investigating tree's physiological response to global change. These latitudinal treeline locations with intermittent forest cover and continuous permafrost are within the northern range limit of white spruce. The sites sampled were located on riverside terraces, and the soils were characterized as cryosols developed on till and glaciofluvial materials resulting from the last glaciation (Jones et al., 2009). Both sites featured mesic conditions and were dominated by white spruce, with no visible sign of drought stress or major disturbance caused by fires or insect infestation (D'Arrigo et al., 2009). These treeline locations were chosen because of the occurrence of old stunted white spruce stands typical of the Arctic tundra open woodland ecosystems present along the Coppermine and Thelon River. The Coppermine and Thelon River areas feature broadly similar subarctic climatic conditions. Mean annual temperature and mean annual precipitation for the study period as measured from 1901 to 2004 were −11.4°C and 227 mm and −11.8°C and 252 mm, respectively (Figure S1 in Supporting Information S1, see Section 2.3 for the gridded climate data used). Average snow depth (September–May) for the period 1961–1990 was 17 cm at Coppermine and 35 cm at Thelon based on the closest meteorological station of Environment Canada located at Cambridge Bay (ca. 75 km from Coppermine) and Baker Lake (ca. 400 km from Thelon), respectively. Active layer thickness data was not available for the study sites. However, according to recent estimates, no significant changes in active layer thickness were reported for the period 1991–2018 across our study region (Smith et al., 2022).

2.2. Tree-Ring Chronology Development

Sampling of 23 and 24 healthy and dominant white spruce trees took place in the summers of 2004 (Coppermine) and 2005 (Thelon), respectively. Two 5 mm diameter increment cores from each tree were obtained and brought to the Tree Ring Lab of the Lamont-Doherty Earth Observatory for dendrochronological analysis. Increment cores were first mounted on wooden supports and successively sanded with finer grades of sandpaper up to 600 grits until the ring boundaries could be clearly distinguished under a stereomicroscope. In 2016, the samples were scanned at a resolution of 3,200 dpi using a color calibrated Epson V850 Pro scanner and the SilverFast Ai IT8 imaging software (Version 8) and the tree-ring widths were measured using the software CooRecorder 9.3 (Cybis Electronik 2019). Ring width was measured to 0.001 mm (0.0038px) precision and cross-dated to ensure accurate calendar dating using dendrochronological methods against the original chronology available at the International Tree-Ring Data Bank: Jacoby - Coppermine River 2003 update - PCMA - ITRDB CANA314 (https://doi.org/10.25921/kpe9-5c53) and Jacoby - Thelon - PCGL - ITRDB CANA318 (https://doi.org/10.25921/ph8v-2c22). The Coppermine and Thelon original tree-ring width and maximum latewood density chronologies were previously used in reconstructions and analyses of Northern Hemisphere annual temperatures, as well as regional temperatures (D'Arrigo et al., 2009, 2006). The Coppermine and Thelon tree-ring width chronologies used in this work span the periods 1676–2003 and 1661–2004, respectively (Table 1, Figure S2 in Supporting Information S1).

For the work presented here, we measured for the first time $\delta^{13}C$ and $\delta^{18}O$ on five selected trees for each site from 1900 to 2003/2004 (Figure S3 in Supporting Information S1). To ensure that the number of trees sampled was

Table 1
Description of the Tree-Ring Chronologies

Site	Nb. trees (ring width)	Ring width span	Rbar	EPS	Nb. trees (isotopes)	$\delta^{13}C$ and $\delta^{18}O$ span	Rbar $\delta^{13}C$	EPS $\delta^{13}C$	Rbar $\delta^{18}O$	EPS $\delta^{18}O$
Coppermine	23	1676–2003	0.32	0.89	5	1900–2003	0.67	0.91	0.52	0.85
Thelon	24	1661–2004	0.31	0.88	5	1900–2004	0.72	0.93	0.53	0.86

sufficiently representative of the sampled population, we calculated the mean interseries correlation between all the series from the different trees (Rbar) and the Expressed Population Signal (EPS, Table 1; Wigley et al., 1984). For the 20th century, all tree-ring chronologies showed EPS values ≥0.85, which is considered the threshold value for adequately reflecting a common signal among trees (Wigley et al., 1984; Table 1).

To detect long-term changes in growth and remove potential age-related effects that can bias growth trends, we detrended the individual crossdated ring-width series using a single-curve Regional Curve Standardization (RCS) method (Peters et al., 2015; Sullivan et al., 2016). To assess long-term growth changes and overcome the problem of declining tree-ring width with increases in tree diameter, we also converted the individual raw tree-ring width series to basal area increments (BAI), which represents the annual change in cross-sectional area of a tree stem (Visser, 1995). The potential age-related trends of the BAI series were further removed using the same RCS procedure as mentioned above.

2.3. Climate and Sea Ice Data

For the period 1901–2004, gridded temperature, precipitation, and cloud cover data sets were used due to the lack of meteorological stations with long temporal records near the study sites. We obtained mean monthly temperature and cloud cover data (0.5° resolution) from the Climate Research Unit (CRU, version TS 4.04; Harris et al., 2020). We also used monthly gridded precipitation data version 7 (0.5° resolution) from the Global Precipitation Climatology Center (GPCC; Becker et al., 2013; Schneider et al., 2018). The use of the GPCC precipitation data was preferred over the CRU TS 4.04 data because it uses the largest gauge-observation data set with the highest reliability prior the 1930s (Sun et al., 2018).

Gridded monthly sea ice extent data (0.25° resolution) were downloaded from the National Snow and Ice Data Center for the period 1850–2017 (Walsh et al., 2019). The data set is based on two data sources: (a) historical observations from ships, reports from oceanographers, and airborne surveys by the national ice services before 1979 and (b) satellite passive microwave data after 1979. These data sources were combined and merged to a uniform gridded product (Walsh et al., 2017). Sea ice extent prior to 1979 may contain uncertainties in absolute values because historical observations are more prone to error bias than satellite-based data (Walsh et al., 2017), but this bias did not affect our analyses, which focused on the influence of interannual variability in sea ice extent on yearly changes in tree-ring variables. We used monthly and mean summer (June–August) Northern Hemisphere sea ice extent in further analyses. Northern Hemisphere sea ice extent data were used instead of sub-regional sea ice extent data sets because correlation coefficients between sea ice extent and tree-ring variables were the highest. The Northern Hemisphere sea ice extent data set covers the 16 Arctic sub-regions according to the Multisensor Analyzed Sea Ice Extent for the Northern Hemisphere: Beaufort Sea, Chukchi Sea, East Siberian Sea, Laptev Sea, Kara Sea, Barents Sea, Greenland Sea, Baffin Bay and Gulf of St. Lawrence, Canadian Archipelago, Hudson Bay, Central Arctic Ocean, Bering Sea, Baltic Sea, Sea of Okhotsk, Yellow Sea, and Cook Inlet (Walsh et al., 2019). The use of the Northern Hemisphere over sub-regional sea ice extent data was further justified by the fact that changes in sea ice extent in the Northen Hemisphere alter global atmospheric circulation, influencing air temperature, precipitation patterns, and storm track behavior across the Arctic (Budikova, 2009).

Since we were interested in assessing the growth and physiological responses of white spruce to concomitant changes in temperature and sea ice extent that occurred in three distinct periods (1900–1940, 1941–1970, 1971–2003/2004), we did not detrend the climate and sea ice data to include the long-term trends in the analyses. Removing the long-term trends in the environmental variables, and thus focusing the analysis solely on the high-frequency (year-to-year variability) would have overlooked the effects of declining sea ice and increasing temperature over the 20th century.

2.4. Isotopic Analysis

At both sites, five tree samples older than 200 yr old, which were used for tree-ring width analysis and had the high correlations with the mean tree-ring width chronology, were selected for isotopic analysis. Each annual ring between 1900 and 2003/2004 was split off with a scalpel under a stereomicroscope and the cellulose was extracted following standard procedures using a high-yield cellulose extraction system (Andreu-Hayles et al., 2019). The α-cellulose was homogenized using an ultrasound bath and then freeze-dried for 24 hr using a vacuum freeze-drier. For each sample, 200 µg of α-cellulose were weighted and placed into silver capsules. The $\delta^{13}C$ and $\delta^{18}O$ ratios were measured simultaneously using high-temperature pyrolysis in a High-Temperature Conversion Elemental Analyzer (TC/EA) coupled to a Thermo Delta plus mass spectrometer at the Geochemistry Laboratory of the Lamont-Doherty Earth Observatory of Columbia University (Andreu-Hayles et al., 2019). The analytical precision for the in-house α-cellulose standards was ±0.15‰ for $\delta^{13}C$ and ±0.26‰ for $\delta^{18}O$.

Raw tree-ring $\delta^{13}C$ values were used to calculate carbon discrimination values ($\Delta^{13}C$) following Farquhar et al. (1982):

$$\Delta^{13}C = \frac{\delta^{13}C_{Air} - \delta^{13}C_{TR}}{1 + \delta^{13}C_{TR}/1,000} \quad (1)$$

where $\delta^{13}C_{Air}$ is the estimated isotopic value of atmospheric CO_2 at time t from McCarroll and Loader (2004) and $\delta^{13}C_{TR}$ is the isotopic value of tree-ring cellulose at time t. According to Farquhar et al. (1982), $\Delta^{13}C$ is linearly related to the ratio of intercellular (c_i) to atmospheric (c_a) CO_2 mole fractions following:

$$\Delta^{13}C \cong a + (b - a) \cdot \left(\frac{c_i}{c_a}\right) \quad (2)$$

where a (4.4‰) is the fractionation during CO_2 diffusion between the ambient atmosphere and the intercellular spaces (O'Leary, 1981), and b (27‰) is the fractionation during carboxylation by Rubisco in C_3 plants. Note that $\Delta^{13}C$ should be directly related to [CO_2] in chloroplasts rather than c_i, making it sensitive to mesophyll conductance (Seibt et al., 2008). Because there is no information on mesophyll conductance of the investigated trees, using mean values from the literature would not improve the interpretations of our tree-ring carbon isotopic data. Therefore, we considered canopy integrated variation in mesophyll conductance to have been negligible. We derived c_i from the following equation:

$$c_i = c_a \frac{\left(\delta^{13}C_{Air} - \delta^{13}C_{TR}\right) - a}{b - a} \quad (3)$$

Intrinsic water-use efficiency ($_i$WUE) of the individual trees, which corresponds to the ratio of assimilation (A), to stomatal conductance (g_s) rates, can be estimated over time according to Farquhar and Richards (1984) from values of $\Delta^{13}C$ and c_a as follows:

$$_iWUE = \frac{A}{g_s} = \frac{c_a\left(b - \Delta^{13}C\right)}{1.6(b - a)} \quad (4)$$

where 1.6 is the ratio of diffusivities of water vapor and CO_2 in the air. We used the c_a values compiled by McCarroll and Loader (2004).

2.5. Data Analysis

We assessed temporal trends in temperature, precipitation, and sea ice extent data for the three aforementioned time periods. For this study, the most recent warming period (1971 to now) ends in 2003 or 2004 corresponding to the last year of tree-ring measurements. Trends were also evaluated for the entire period of analysis (1901–2003/2004). We applied Mann-Kendall trend tests and calculated Sen's slope estimates from prewhitened climate time series (i.e., temporal autocorrelation removed before computation) following Yue et al. (2002) with the R package *zyp* (Bronaugh & Werner, 2019).

We used the three theoretical scenarios of leaf-gas exchange strategy proposed by Saurer et al. (2004) to interpret possible physiological responses and changes in $_i$WUE over time. In scenario (a), trees maintain a constant

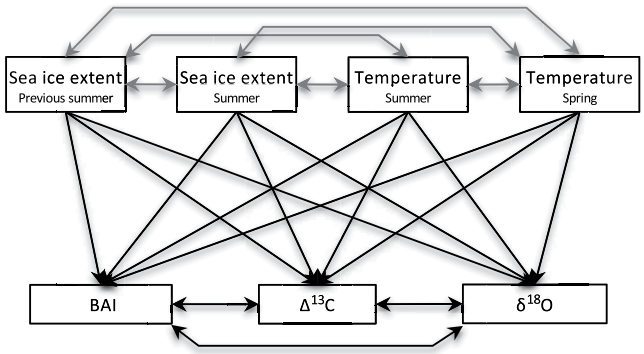

Figure 2. Structural equation model used for assessing the influence of spring (March–May) and summer (June–August) temperature and sea ice extent on undetrended basal area increment (BAI), $\Delta^{13}C$, and $\delta^{18}O$ tree-ring records. Single-headed arrows denote causal relationships and double-headed arrows indicate covariation between variables. Gray arrows denote covariation between explanatory variables.

c_i, with a strong increase in stomatal regulation, hence $_i$WUE increases strongly. In scenario (b), trees keep a constant c_i/c_a ratio with a moderate increase in stomatal regulation, which leads to a moderate increase in $_i$WUE. In scenario (c), the difference between c_a and c_i remains constant with no changes in stomatal regulation, and consequently $_i$WUE remains constant.

We assessed the significance of the changes in BAI, $\Delta^{13}C$, $_i$WUE, and $\delta^{18}O$ between the three periods (1901–1940, 1941–1970, 1971–2003/2004) using probability density functions and nonparametric Kolmogorov-Smirnov tests to take into account the different number of years between the periods. To assess the relative influence of the physiological controls (i.e., A and/or g_s) on tree response to year-to-year climate variability, we first removed the long-term trends in the isotopic time series and retained the high frequency by calculating the year-to-year differences. We then correlated the $\Delta^{13}C$ and $\delta^{18}O$ year-to-year differences for the three periods to assess how A and/or g_s varied in periods with contrasting climatic conditions.

To assess the environmental signals recorded in the tree-ring variables, bootstrapped correlation coefficients were calculated between BAI, $\Delta^{13}C$, $\delta^{18}O$ and mean monthly temperature, precipitation amount, cloud cover, and sea ice extent with the R package *treeclim* (Zang & Biondi, 2015) for 1901–2003 (Coppermine) and 1901–2004 (Thelon). Correlations were calculated from June of the year prior to ring formation to September of the year of ring formation. We identified the seasons of the year with the strongest significant correlations between the tree-ring and environmental variables: temperature (Figure S4 in Supporting Information S1), precipitation (Figure S5 in Supporting Information S1), sea ice extent (Figure S6 in Supporting Information S1) and cloud cover (Figure S7 in Supporting Information S1). Boostrapped moving correlations were also calculated between mean summer temperature, precipitation sum, sea ice extent, and the tree-ring variables (Figure S8 in Supporting Information S1). Based on these analyses, mean spring (March–May) and summer (June–August) temperatures, and summer sea ice extent were selected for inclusion in structural equation models (below; Figure 2).

We assessed growth and gas exchange responses to simultaneous changes in temperature and sea ice extent by performing piecewise structural equation modeling (SEM) using the R package *piecewiseSEM* (Lefcheck, 2016). Piecewise SEMs are advanced multivariate statistical techniques that can be used with small sample sizes and that allow for the inclusion of random effects and different correlation structures. For each site and study period, we developed a piecewise SEM to assess the combined effects of spring and summer temperature, and previous and current summer sea ice extent on BAI, $\Delta^{13}C$, and $\delta^{18}O$ measurements (Figure 2). We used a linear mixed effects model structure (Zuur et al., 2009) within each SEM to assess both the fixed effects (spring and summer temperature, and previous and current summer sea ice extent) and random effects (individual tree series) on tree-ring variables using the function *lme* from the *nlme* package (Pinheiro et al., 2013). We also accounted for temporal autocorrelation in time series by including an autoregressive process of order 1 in the models. The SEMs were fit for the periods 1901–1940, 1941–1970, and 1971–2003. We assessed the model fit with Fisher's C statistic and Akaike's information criterion (Lefcheck, 2016).

3. Results

3.1. Climatic and Sea Ice Extent Trends

The analysis of the CRU TS 4.04 gridded temperature data indicated three periods with distinct temperature trends at both study sites in summer (Figures 3a and 3b) and annually (Figures S1a and S1b in Supporting Information S1). First, a warming period occurred between 1900 and 1940. During this period, a significant increase in mean summer (June, July, August) temperature of +0.02°C/yr at Coppermine and +0.04°C/yr at Thelon was recorded. Second, a period with a slight cooling trend, albeit not significant, happened between 1941 and 1970. The third and ongoing period since the 1970s corresponds to the late century anthropogenic warming and is characterized by a steady increase in mean annual temperature of +0.04°C/yr (+0.02°C/yr in summer) at both sites. Over the period 1901–2004, mean annual temperature increased by 1.1°C at Coppermine and 1.0°C at Thelon.

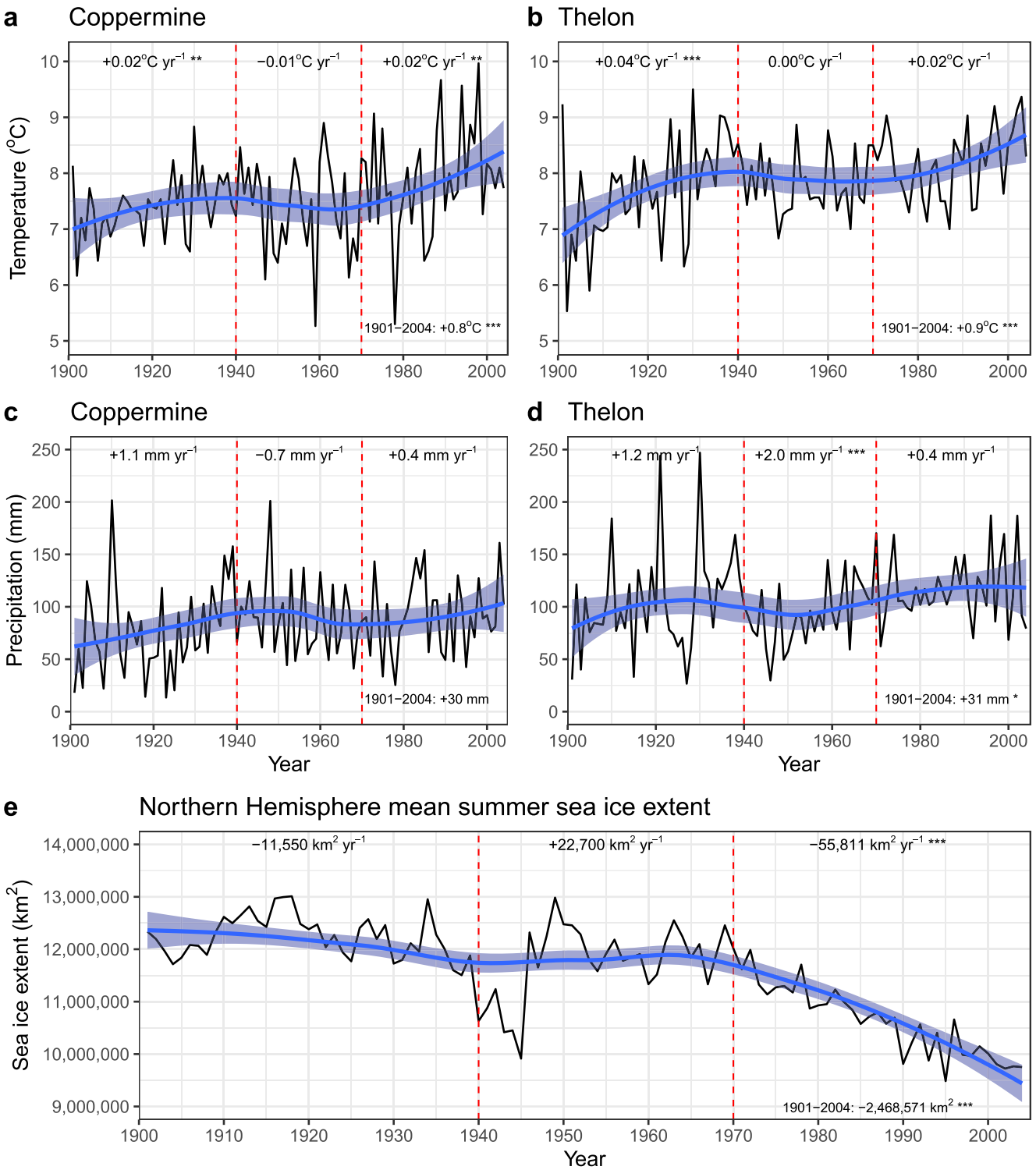

Figure 3. Mean summer temperature (a, b) and precipitation sum (c, d) at Coppermine and Thelon for the period 1901–2004. In (e), mean summer sea ice extent for the Northern Hemisphere for the period 1901–2004. The 20th century trends are indicated by the blue smoothed lines with 95% confidence interval. The vertical red dotted lines indicate the early 20th century (1901–1940) and recent (1970–2004) warming periods. Trends for each period were assessed with Mann-Kendall trend tests and are indicated in inset. Significance levels: ***$P < 0.001$; **$P < 0.01$; *$P < 0.05$.

The analysis of the gridded GPCC precipitation data indicated a high year-to-year variability at Coppermine and Thelon in summer (Figures 3c and 3d) and annually (Figures S1c and S1d in Supporting Information S1). At both sites, no significant trends in summer precipitation were detected for the three periods separately, except the small increase (+2.0 mm/yr) recorded at Thelon for the period 1941–1970. Between 1901 and 2004, annual precipitation increased by 46 mm at Coppermine and 61 mm at Thelon, but these increases were not statistically significant (Figures S1c and S1d in Supporting Information S1).

Summer sea ice extent in the Arctic did not show significant trends between 1901 and 1970 (Figure 3e). However, between 1970 and 2004, summer sea ice extent significantly declined by 55,811 km^2 per year. Over the period 1901–2004, pan-Arctic summer sea ice extent significantly declined by 2,468,571 km^2.

3.2. Changes in Tree Growth, $\Delta^{13}C$, $_{i}WUE$, and $\delta^{18}O$ Over the Last Century

We found contrasting growth trends for white spruce at the two treeline sites over the last three centuries (Figures 4a and 4b, Figure S2 in Supporting Information S1). At the site located closer to the Arctic Ocean (Coppermine) BAI steadily increased between 1900 and 2003, whereas at the more interior site (Thelon) BAI increased from 1900 to ca. 1925, remained stable for the period 1925–1950, and then declined. BAI significantly increased from the earliest to the latest period at Coppermine (1900–1940, mean 1.5 cm^2/yr; 1941–1970, mean 1.8 cm^2/yr; 1971–2003, mean 2.0 cm^2/yr; Figure 5a). At Thelon, BAI was significantly lower in 1971–2003 than in the former periods (Figure 5b). These contrasting growth trends were even more pronounced when we looked at the full time length of the raw tree-ring width and BAI chronologies (Figure S2 in Supporting Information S1). At Coppermine, growth continuously increased between 1750 and 2003, except during the Little Ice Age when a reduction in BAI occurred in the early to mid-1800s. At Thelon, we found variable growth trends characterized by a steep increase in BAI in the late 18th century, reduced BAI during the Little Ice Age period, a strong increase in BAI between the end of the 19th century until ca. 1925, and a steady decline in BAI after 1950. For the period 1901–2003, the Coppermine and Thelon BAI index chronologies correlated moderately ($r = 0.32$, $P < 0.001$).

Besides these changes in growth, we also found long-term changes in tree-ring isotopic records during the 20th century (Figures 4 and 5, Table S1 and Figure S3 in Supporting Information S1). At both sites, $\Delta^{13}C$ slightly increased over time (Figures 4c and 4d and Figures 5c and 5d). The $_{i}WUE$ showed no significant trend until ca. 1970 but significantly increased after (Figures 4e and 4f), leading to significantly higher $_{i}WUE$ in 1971–2004 than in the 1900–1940 and 1941–1970 periods (Figures 5e and 5f). From 1971 to 2004, $_{i}WUE$ significantly increased by 11% and 12% at Coppermine and Thelon, respectively. When compared to simulated baseline scenarios of $_{i}WUE$, the $_{i}WUE$ trends at both sites laid in-between the constant $c_a - c_i$ scenario and after 1970 the c_i/c_a scenario (Figures 4e and 4f). At Coppermine, $\delta^{18}O$ steadily rose after 1970 whereas at Thelon no trends in $\delta^{18}O$ occurred over time, except for the lower $\delta^{18}O$ values reported for the period 1941–1970 (Figures 4g and 4h, Figures 5g and 5h). The mean $\delta^{18}O$ values for the period 1900–2004 were lower at Coppermine (18.27‰ ± 1.19‰) than at Thelon (19.26‰ ± 1.01‰).

3.3. Environmental Signals Recorded in Tree-Ring Variables

Previous and current summer temperature and sea ice extent, and spring temperature had the strongest influence on tree-ring variables over the three time periods (Figures S4 and S6 in Supporting Information S1). The tree-ring variables did not record a clear precipitation signal (Figure S5 in Supporting Information S1), except for the shift from positive to negative correlations between summer precipitation and $\delta^{18}O$ at Thelon (Figure S8f in Supporting Information S1). In contrast, we found positive correlations between BAI and summer temperature for the periods 1901–1940 and 1941–1970 at Coppermine and Thelon. These positive correlations with summer temperatures became non-significant or even negative for the period 1971–2003 at Thelon, while Coppermine kept positive albeit non-significant positive correlations (Figures S4 and S8 in Supporting Information S1). Tree-ring $\Delta^{13}C$ was negatively correlated to May–August temperature after 1940 (Figure S4 in Supporting Information S1). While $\Delta^{13}C$ showed stable significant negative correlations with summer temperature at Coppermine over the 20th century, correlations between $\Delta^{13}C$ and summer temperature at Thelon became negatively stronger after 1940 (Figures S8c and S8d in Supporting Information S1). Tree-ring $\delta^{18}O$ was essentially positively correlated to temperatures during the early 20th century warming period (1901–1940) and late-century warming period (1971–2003) at both sites, whereas positive and negative correlations were observed for the 1941–1970

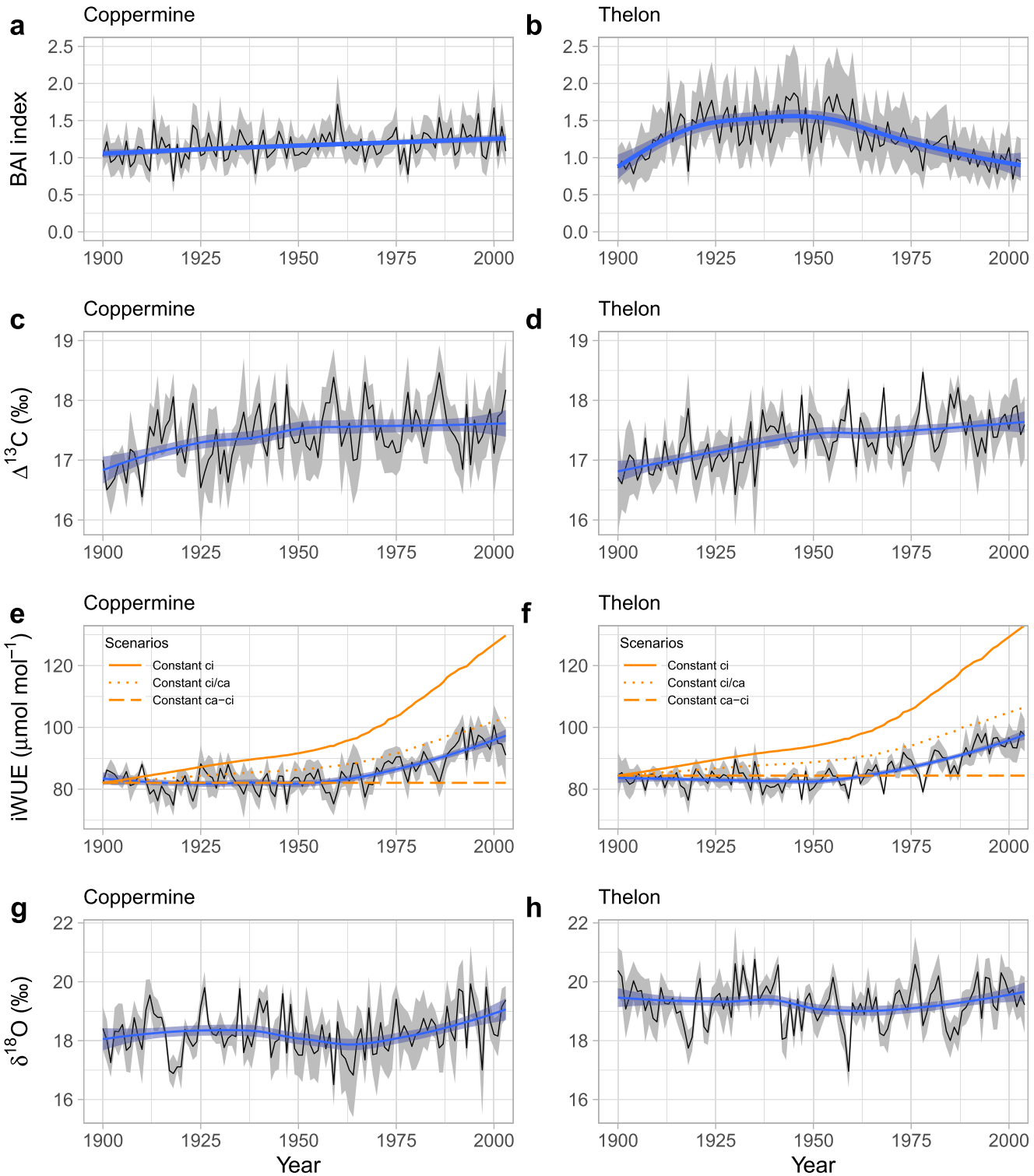

Figure 4. Basal area increment (BAI) standardized chronologies (regional curve standardization; (a, b)), carbon isotope discrimination ($\Delta^{13}C$; (c, d)), intrinsic water-use efficiency ($_{i}$WUE; (e, f)), and $\delta^{18}O$ (g, h) of white spruce trees for the period (1900–2003/2004) at Coppermine and Thelon. In (e and f), the three theoretical $_{i}$WUE scenarios according to Saurer et al. (2004) reflecting specific leaf gas exchange response to changing c_a are shown. The gray shading indicates the 95% bootstrapped confidence limit of the mean. Smoothed means are shown as blue lines. Trends for the tree-ring variables for the periods (1900/1901–1940, 1941–1970, and 1971–2003/2004) are available in Table S1 in Supporting Information S1.

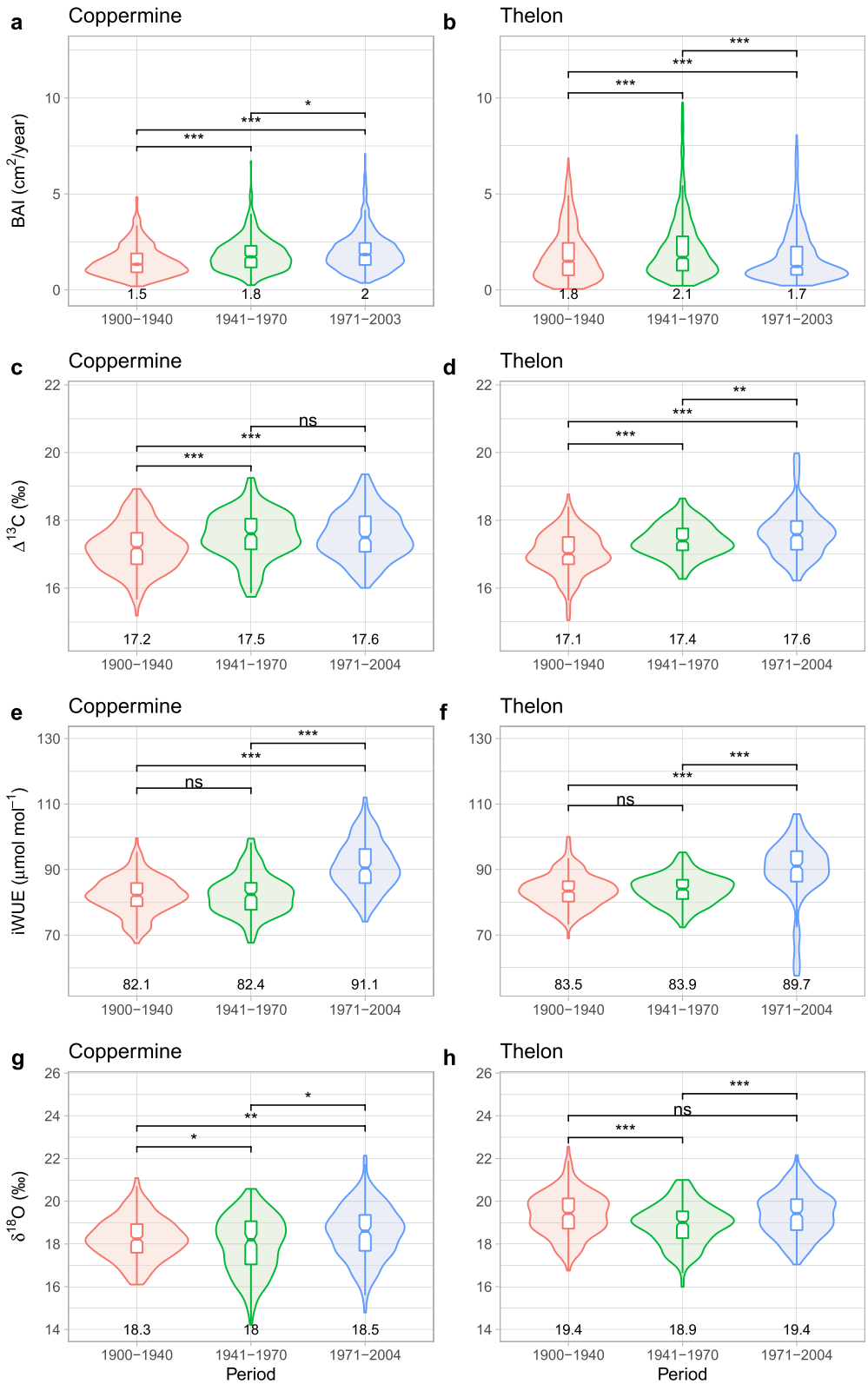

Figure 5. Violin plots show the probability density of the raw tree-ring data for the three periods. The box plots show the median and the interquartile range of the data. Mean values for each period are indicated under the plots. Significant differences between the periods were assessed with Kolmogorov-Smirnov tests. Significance levels: ***$P < 0.001$; **$P < 0.01$; *$P < 0.05$; ns, non-significant.

period (Figure S4 in Supporting Information S1). At Coppermine, $\delta^{18}O$ was significantly positively correlated to May–June (1941–1970) and April–June (1971–2003) temperatures. When looking at the moving correlations between $\delta^{18}O$ and summer temperatures, positive correlations were stronger after ca. 1970 at Coppermine, while at Thelon, the strength of the correlations declined over the 20th century (Figures S8e and S8f in Supporting Information S1).

Regarding the influence of sea ice on tree-ring variables (Figure S6 in Supporting Information S1), BAI at Thelon was strongly negatively correlated to previous summer, previous fall, and current summer sea ice extent for the period 1941–1970 and strongly positively correlated to sea ice extent between 1971 and 2003. The moving correlation analysis further supported this shift from negative to positive correlations between BAI and summer sea ice extent at Thelon in the 20th century (Figure S8b in Supporting Information S1). Tree-ring $\Delta^{13}C$ did not show any clear pattern for sea ice extent. Tree-ring $\delta^{18}O$ was mostly negatively correlated with sea ice extent at both sites over the three periods. Especially, previous summer sea ice extent was strongly negatively associated with tree-ring $\delta^{18}O$ at Coppermine for the period 1941–1970 and 1971–2003. Cloud cover only significantly correlated from June to August with $\Delta^{13}C$ at Thelon (Figure S7 in Supporting Information S1).

3.4. Growth and Physiological Responses of White Spruce to Concomitant Changes in Temperature and Sea Ice Extent

When simultaneously analyzing the effects of temperature and sea ice extent on tree-ring variables with piecewise SEMs, we found unstable effects of environmental factors over time as indicated by the changes in regression (β) coefficients (Figure 6). At Coppermine, summer temperatures had a positive influence on BAI in 1901–1940 ($\beta = 0.15$, $P < 0.001$) and 1941–1970 ($\beta = 0.25$, $P < 0.001$), and had a negative effect in 1971–2003 ($\beta = -0.22$, $P < 0.001$). Spring temperatures had a negative effect on BAI only in 1971–2003 ($\beta = -0.24$, $P < 0.001$). We found a stable significant negative effect of summer temperature on $\Delta^{13}C$ over the three periods at Coppermine (Figures 6a, 6c, and 6d), which was absent at Thelon (Figures 6b, 6d, and 6f). The absence of negative responses of $\Delta^{13}C$ to summer temperatures in the SEMs for the most recent period at Thelon disagreed with the results from the moving correlations analysis, that is, strong and significant negative correlations between 1940 and 2000 (Figure S8d in Supporting Information S1).

Previous summer sea ice extent had a stronger significant negative influence on $\delta^{18}O$ at Coppermine than Thelon for the period 1941–1970 ($\beta = -0.37$, $P < 0.001$ vs. -0.25, $P = 0.005$) and 1971–2003 ($\beta = -0.40$, $P < 0.001$ vs. -0.14, $P = 0.060$). At Thelon, the effect of current summer sea ice extent on $\Delta^{13}C$ shifted from positive in 1901–1940 ($\beta = 0.17$, $P = 0.017$) to negative in 1940–1970 ($\beta = -0.31$, $P < 0.001$) and 1971–2003 ($\beta = -0.25$, $P = 0.002$). At Coppermine, the influence of current summer sea ice extent over $\Delta^{13}C$ was negative for the two last periods 1941–1970 and 1971–2003 ($\beta = -0.16$, $P < 0.001$).

We found negative covariation between $\Delta^{13}C$ and $\delta^{18}O$ for the different periods for Thelon but not for Coppermine (Figure 6). In agreement, the negative correlations between the year-to-year differences in $\Delta^{13}C$ and $\delta^{18}O$ were stronger for Thelon than Coppermine, with the exception of the periods 1941–1970 and 1971–2003 in which they were similar (Figures 7c and 7d). Significant, stable, and negative correlations between the year-to-year differences in BAI and $\Delta^{13}C$ were found at Thelon, but not at Coppermine (Figures 7a and 7b). BAI and $\delta^{18}O$ year-to-year differences correlated positively at both sites, but the correlation strength varied between the periods (Figure S9 in Supporting Information S1).

4. Discussion

Ongoing climate warming is profoundly altering physiology, growth, and productivity of northern treeline spruce forests (Beck et al., 2011; Sniderhan et al., 2021; Wilmking et al., 2004). Our results and other studies, however, indicate that these changes in forest growth are not linear in time, nor are they coherent across the Arctic.

4.1. Contrasting Radial Growth Response at Two Remote Latitudinal Treeline Sites

While we found a steady and slight increase in tree growth at Coppermine, growth has been declining at Thelon. Many studies have reported contrasting growth responses to temperature and divergent growth trends in high-latitude spruce dominated forests over the 20th century (e.g., McGuire et al., 2010; Porter & Pisaric, 2011;

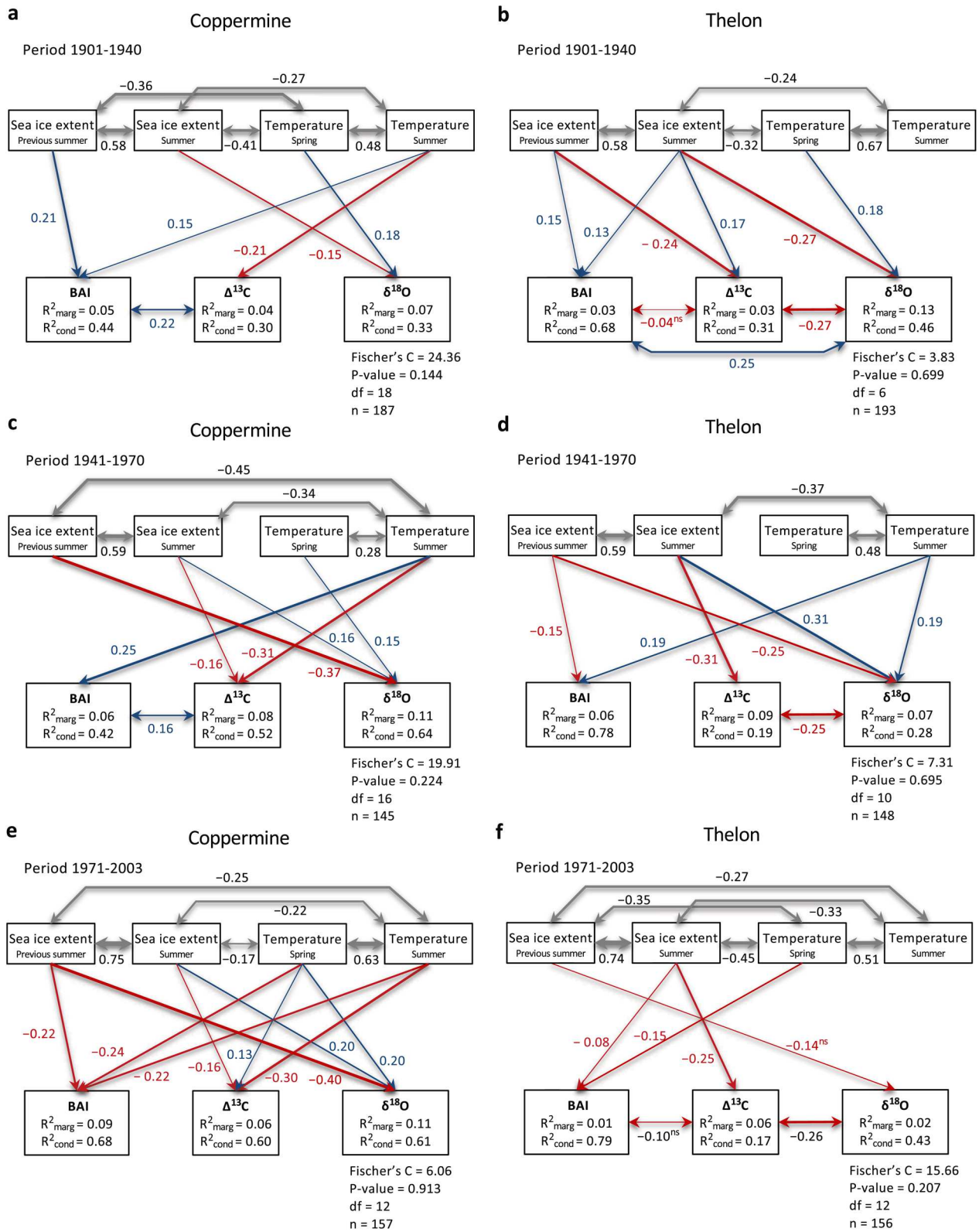

Figure 6.

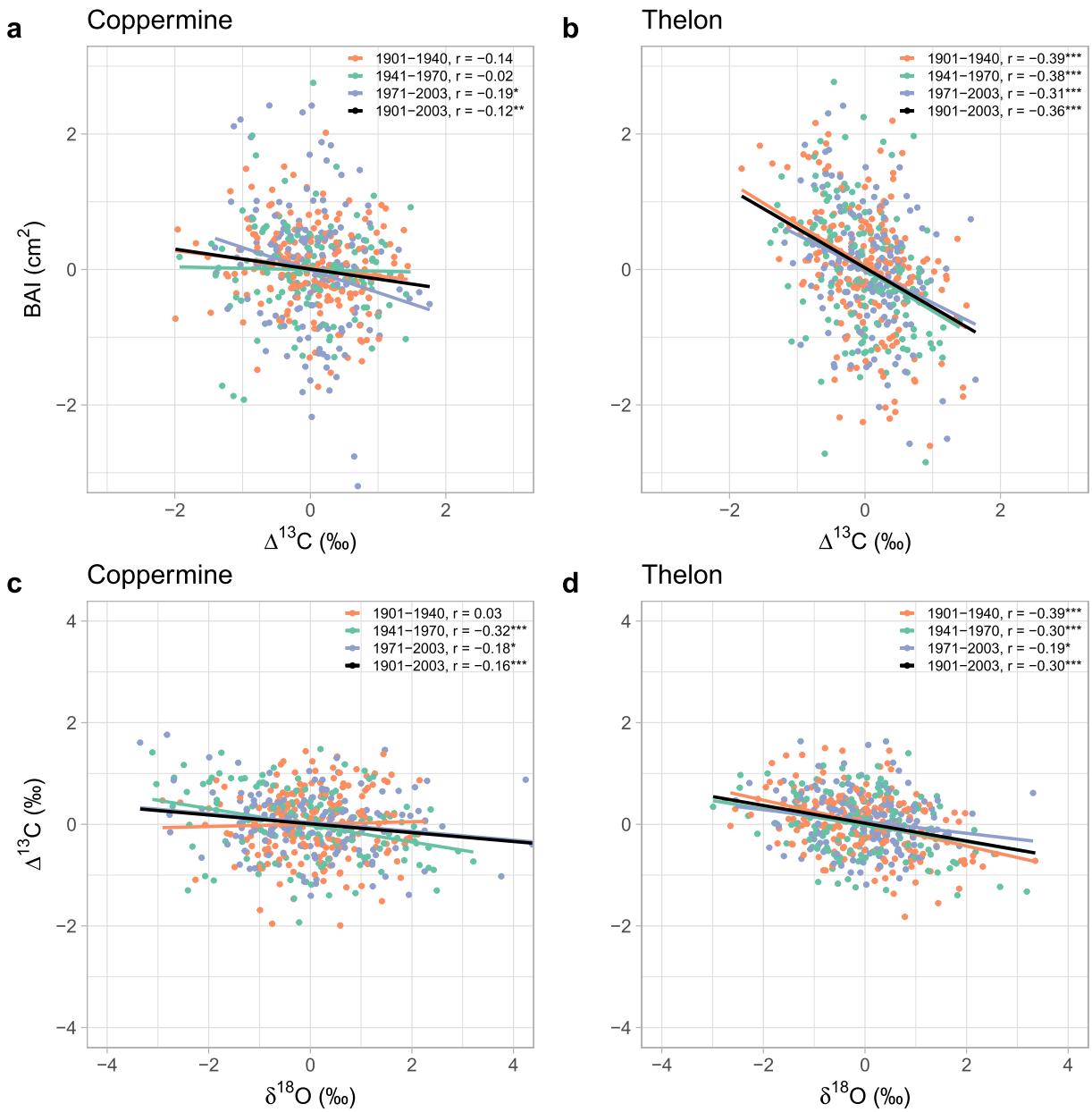

Figure 7. Correlations between year-to-year differences in basal area increment, $\Delta^{13}C$, and $\delta^{18}O$ measured in tree rings of five spruce trees for the distinct periods 1901–1940, 1941–1970, 1971–2003, and the whole period 1901–2003 at Coppermine (a, c) and Thelon (b, d). Significance levels: ***$P < 0.001$; **$P < 0.01$; *$P < 0.05$.

Sniderhan & Baltzer, 2016; Sullivan et al., 2017; Wilmking et al., 2004). While some authors reported that warming-induced drought stress during the 20th century has led to growth reduction of white spruce in high-latitude boreal forests of North America (Barber et al., 2000; McGuire et al., 2010), others found limited

Figure 6. Fitted piecewise structural equation models showing the relative influence of spring and summer temperature, and previous summer and current summer sea ice extent on undetrended basal area increment (BAI), $\Delta^{13}C$, and $\delta^{18}O$ of white spruce trees at Coppermine and Thelon for the periods 1901–1940 (a, b), 1941–1970 (c, d), and 1971–2003 (e, f). Single-headed arrows indicate causal relationships and double-headed arrows denote covariation between variables. The width of arrows is proportional to the strength of path coefficients. Standardized regression coefficients are indicated next to the paths. All coefficients are significant ($P < 0.05$) except those with ^{ns} that were kept in the model because they improved the model fit. Blue and red paths indicate positive and negative effects, respectively. Gray paths indicate covariation between explanatory variables. Amount of variance explained by the fixed effects only (R^2_{marg}) and by the fixed and random effects (R^2_{cond}) are listed for each response variable. The model fit was evaluated using Shipley's test of *d*-separation. A Fisher's C statistic with a *P*-value >0.05 indicate that no paths are missing, and the model is a good fit. The degree of freedom (df) and number of observations (*n*) are also shown. Summary statistics for each single linear mixed-effects model used in the piecewise structural equation models are reported in Table S2 in Supporting Information S1).

evidence of declining growth among spruce populations (Sullivan et al., 2017) and even enhanced growth in the last decades of the 20th century (Andreu-Hayles et al., 2011a). Regarding climate sensitivity, at both sites tree growth (BAI) was positively influenced by summer temperature until 1970 when this relationship became non-significant or negative, suggesting the emergence of the divergence phenomenon as already reported at white spruce sites in Yukon (Porter & Pisaric, 2011), Northwest Territories (Field et al., 2022; Pisaric et al., 2007), and Alaska (Andreu-Hayles et al., 2011a).

The contrasting growth trends between Coppermine and Thelon do not seem driven by different climate conditions since both sites have similar mean annual temperature and precipitation and shared warming trends (+0.04°C/yr since 1970), as well as no-clear precipitation patterns. However, differences in growth responses and trajectories can be caused by variations in landscape and other local or microsite characteristics such as elevation, slope, aspect, upland versus floodplain conditions (Wilmking et al., 2004), permafrost thaw (Nicklen et al., 2021), and/or successional stages (McGuire et al., 2010). Our study sites consisted of late successional stage white spruce forest stands located on riverside terraces along the Coppermine and Thelon River and featured mesic conditions with no recent evidence of drought stress or stand-replacing disturbances such as fires or insect infestation (D'Arrigo et al., 2009). At these sites, it is plausible that warming may have induced permafrost thaw, hence altering soil moisture conditions and tree growth. Recent work indicates that rising summer temperatures can lead to increased radial growth of spruce in areas with deep permafrost thaw or no near-surface permafrost whereas warming can lead to growth declines in areas with near-surface permafrost (Nicklen et al., 2021).

Despite that only sparse information on soil moisture and permafrost conditions was available at the sites, our isotopic results did not show any evidence supporting the hypothesis that permafrost can be the factor driving growth decline at Thelon during the last decades. First, changes in permafrost conditions and soil moisture over time alter the isotopic signature of the soil water and source water of trees (Sugimoto, 2019). Tree source water originating from melted permafrost is isotopically depleted (Saurer et al., 2016; Sugimoto, 2019). Thus, if trees have been increasingly using this water pool, a decline in tree-ring $\delta^{18}O$ time series should be noticed. However, we found a slightly increasing trend in $\delta^{18}O$ at Coppermine in the last decades of the 20th century and no long-term trend in $\delta^{18}O$ time series at Thelon (Figures 4g and 4h, Table S1 in Supporting Information S1). This suggests that at our sites permafrost thawing did not occur or was negligible since an increased uptake of melted permafrost water depleted in $\delta^{18}O$ would have caused a decline in tree-ring $\delta^{18}O$. Therefore, it seems unlikely that the decline in white spruce growth at Thelon was caused by permafrost thaw-driven water stress as reported for black spruce at mid-latitude sites with discontinuous permafrost in northwestern Canada (Patankar et al., 2015; Sniderhan et al., 2021).

Second, warming-induced permafrost thaw leading to active layer thickening would have altered soil moisture conditions by lowering the water table and drying the upper soil layers (Patankar et al., 2015). However, we did not find significant changes in soil moisture content over the period 1979–2004 at both sites according to the satellite-observed soil moisture time series (Text S1 and Figure S10 in Supporting Information S1). A decrease in soil moisture over time would have likely induced drought-induced stomatal closure and caused a reduction in $\Delta^{13}C$, but this was not the case at either site where a slight increase in $\Delta^{13}C$ was observed (see Section 4.2 below).

4.2. $\Delta^{13}C$ and Physiological Responses

Over the last century, white spruce at the two sites shared a slight but significant increase in $\Delta^{13}C$ (Figures 4c and 4d and Figures 5c and 5d). This increase in $\Delta^{13}C$ was accompanied by a minor but continuous increase in BAI at Coppermine, whereas at Thelon BAI increased during the first half of the 20th century and then declined (Figures 4a and 4b).

At Coppermine, the parallel increase in $\Delta^{13}C$ and BAI suggests that carbon assimilation through higher photosynthetic rates and/or stomatal conductance, as well as carbon fixation through wood formation increased over time (Figures 4a and 4c). However, we found no or weak correlations between BAI and $\Delta^{13}C$ at Coppermine (Figure 7a), indicating that radial growth and leaf-level physiological processes (stomatal conductance and photosynthetic rates) were mainly uncoupled. When we compared both isotopes, we observed none or weak negative associations between $\Delta^{13}C$ and $\delta^{18}O$ (Figure 7c), indicating that leaf-level adjustments in stomatal conductance and photosynthetic capacity are reflected by $\Delta^{13}C$, while $\delta^{18}O$ may be potentially more influence by the $\delta^{18}O$ source water signal. The significant negative associations between $\Delta^{13}C$ and summer temperature at Coppermine,

which were stable throughout the three periods (Figures 6a, 6c, and 6e, Figure S8 in Supporting Information S1), indicate that warming may be linked to lower values of $\Delta^{13}C$ that may occur under situations of low stomatal regulation and high c_i. These results do not suggest any potential temperature-induced stomatal closure but rather that rising c_a and/or warming may have favored photosynthetic assimilation rates and growth at Coppermine.

At Thelon, the decoupling between $\Delta^{13}C$ and BAI after 1950 (i.e., $\Delta^{13}C$ increased in the period of growth decline; Figures 4b and 4d) and the negative correlations between BAI and $\Delta^{13}C$ (Figure 7b) suggest that as in Coppermine, xylogenesis and carbon assimilation processes at leaf level may be decoupled. This together with the positive moving correlations between BAI and summer temperature between the 1940s and 1990s (Figure 7b in Supporting Information S1) indicate at first sight that temperature-induced drought stress is unlikely to have caused the growth decline. This is further supported by the lack of significant negative path coefficients in the SEMs between $\Delta^{13}C$ and spring and summer temperatures at Thelon (Figures 6b, 6d, and 6f), suggesting a limited influence of temperature-induced drought stress on stomatal control at this site. However, when we looked solely at the effect of summer temperature on $\Delta^{13}C$ and how it evolved with the moving correlations analysis, we observed a shift from nonsignificant correlations between $\Delta^{13}C$ and temperature prior to 1940 to significant negative correlations after 1940 (Figure 8d in Supporting Information S1). This result suggests increased physiological sensitivity of spruce trees at Thelon to rising temperatures. Using different methods, D'Arrigo et al. (2009) found evidence for potential divergence and drought stress at Thelon, mainly that the correlation with precipitation and ring width increased in the more recent period, while that with temperature declined. Besides the increase in temperature sensitivity, the negative association between $\Delta^{13}C$ and $\delta^{18}O$ at Thelon over the three periods (Figures 6b, 6d, and 6f and Figure 7d) implies a tight physiological control on stomatal conductance reflected by both isotopes as a result of evaporative enrichment at leaf-level that may lead to reduced carbon uptake and growth during unfavorable environmental conditions that are not necessarily temperature driven. For example, the strong positive correlations found between $\Delta^{13}C$ and summer cloud cover at Thelon (Figure S7 in Supporting Information S1) indicate that solar radiation could be a factor that may have exacerbated white spruce climate sensitivity and triggered growth reductions, as reported in interior Alaska (Nicklen et al., 2019), by exerting a control on stomatal conductance and photosynthetic rates.

Overall, these contrasting findings at Coppermine and Thelon indicate that $\Delta^{13}C$ in tree-ring cellulose may not necessarily record temperature-induced drought stress through stomatal regulation, as reported elsewhere in high-latitude spruce forests (Barber et al., 2000) since other environmental variables besides air temperature (e.g., irradiance, air humidity) can influence the $\Delta^{13}C$ signal through adjustments in stomatal conductance and photosynthetic rates (McCarroll & Loader, 2004).

4.3. Moderate Increases in WUE

Over the study period 1901–2003, c_a increased from 297 to 373 ppm. Elevated c_a alters tree carbon-water relationships by causing changes in stomatal conductance and photosynthetic rates (McCarroll & Loader, 2004). At both treeline sites, $_i$WUE remained stable until ca. 1970, indicating a passive stomatal regulation to increased c_a. During this period c_i increased in parallel to the rise in c_a to maintain a constant $c_a - c_i$. After 1970, white spruce trees shifted their gas exchange strategy and exhibited an active stomatal regulation by maintaining a constant c_i/c_a ratio that translated to an increase in $_i$WUE of ~11%–12% at both sites. This limited increase in $_i$WUE of ~11%–12% over the period 1901–2003/2004 contrasts with the average increase of 26% in $_i$WUE found for conifers over the 20th century in Europe (Saurer et al., 2014) and the ~30%–40% increases reported for white and black spruce in North American boreal forests (Beaulne et al., 2021; Sullivan et al., 2017).

The nonlinear trends in $_i$WUE found in our study are in line with the reported shifts from passive to active responses to rising atmospheric c_a and small increases in $_i$WUE observed in the last decades for some high-latitude conifer forests (Saurer et al., 2004, 2014; Voltas et al., 2020). Since $\Delta^{13}C$ slightly increased at both sites over the last century, the increase in $_i$WUE after 1970 was most likely a response to rising c_a than a response to temperature-induced drought stress. A common physiological response of trees under elevated c_a is to reduce stomatal conductance and simultaneously maintain or increase c_i, allowing for conservation of water and enhancement of photosynthetic assimilation rates and growth (McCarroll & Loader, 2004). On the one hand, rising c_a may have buffered white spruce at Coppermine from temperature-induced drought stress by compensating for stomatal closure. On the other hand, it is possible that at Thelon elevated c_a was not enough for compensating stomatal closure driven by warmer temperatures, so that the increase in $_i$WUE may be accompanied by a reduction in growth.

4.4. Effect of Sea-Ice Extent on BAI and Tree-Ring $\delta^{18}O$

In parallel to the changes in photosynthetic assimilation and stomatal conductance rates due to rising c_a, our SEM results indicate that the concomitant changes in temperature and sea ice extent had significant direct and indirect effects (i.e., impact of sea ice decline on regional climate) on tree physiology and growth. The pronounced warming in the Arctic and the widespread decline in sea ice extent have altered ocean-atmosphere moisture flux and led to an increase in evaporation and moisture transport from ocean to inland in the Canadian Arctic in the last few decades (Kopec et al., 2016). In our study region, precipitation that originates from Arctic Ocean evaporation has increased by 18% per 10^5 km^2 sea ice loss (Kopec et al., 2016). These changes in evaporation and moisture sources have altered source water $\delta^{18}O$ signature of our treeline trees. This phenomenon was particularly evident at the site closer to the ocean (Coppermine) where we observed a steady increase in tree-ring $\delta^{18}O$ after 1970 (Figure 4g), suggesting an enrichment in source water $\delta^{18}O$ signature due to more moisture originating from open sea (Faber et al., 2017). This response was further supported by the strong negative correlations between previous summer sea ice extent and tree-ring $\delta^{18}O$ in the most recent periods (1941–1970 and 1971–2003). We did not find such an increase in $\delta^{18}O$ in the last decades at the more interior site (Thelon, Figure 4h) likely because air masses originating from open sea water had little influence on precipitation isotopic signature so far inland. While moisture sources originating from open water exert a strong and direct control on precipitation signature in the Arctic (Mellat et al., 2021) and indirectly on tree-ring $\delta^{18}O$ (Gaglioti et al., 2017), this effect is attenuated as the distance traveled by air masses increases when traveling inland (Dansgaard, 1964). This is well reflected in the average tree-ring $\delta^{18}O$ values that were lower at the more coastal site Coppermine (18.27‰) than at the interior site Thelon (19.26‰).

Disentangling temperature versus sea-ice extent effects on tree-ring isotopes and BAI is challenging because summer sea-ice extent correlates negatively with spring and summer air temperatures and these correlations were not stable over the last century (Figure 6, Figure S8 in Supporting Information S1). The regression coefficients of the SEMs indicate that spring temperatures exerted a stronger negative effect on current summer sea-ice extent during the warm periods (1901–1940, 1971–2003) than during the cool period (1941–1970). Air temperature has a direct effect on sea ice extent, which amplifies cooling and warming through albedo effects and influences moisture sources and transport (Serreze et al., 2007). We found the lowest tree-ring $\delta^{18}O$ values at both sites during the coolest period of the 20th century (1941–1970) when summer sea ice covered a much larger area in the Arctic than in the late century warming period (1971–2003) (Chapin et al., 2005). When we simultaneously considered temperature and sea ice effects and their interactions on tree-ring variables in SEMs, sea-ice extent had a significant effect on tree-ring $\delta^{18}O$ at Coppermine but not at Thelon during the most recent period (1971–2003). This difference between the two sites reemphasizes the stronger influence of open-water and sea-ice conditions on tree-ring $\delta^{18}O$ of treeline trees located closer to the Arctic Ocean than those from more interior sites as reported elsewhere in the Arctic (e.g., Gaglioti et al., 2017; Saurer et al., 2002). This extra moisture source due to more open sea could also be a factor behind the contrasting growth trends since white spruce at the Coppermine site may receive more moisture than at Thelon.

Taken together, our results indicate complex and nonlinear responses of treeline trees to the concomitant changes in air temperature, sea-ice extent, and rising c_a over the last century. While our SEM analysis helps to disentangle the relative influence of temperature and sea-ice extent on growth and physiology during the period with contrasting temperatures, the interpretation of our SEM results is not straightforward and should be taken with caution. Still, this approach may be more appropriate than simple correlation analysis because SEM analysis considers covariations between explanatory and response variables.

5. Conclusions

We investigated the growth and physiological responses of white spruce to climate warming and decline in sea ice extent at two latitudinal treeline sites over the 20th century based on annually resolved tree-growth and isotopic data. The sampled sites consisted of old-growth undisturbed white spruce stands located on riverside terraces and representative of the Coppermine and Thelon river Arctic ecosystems, two remote regions with a scarcity of long-term growth and isotopic data. We found different growth trends between the two sites but similar $\Delta^{13}C$ and $_{i}WUE$ trajectories of white spruce over the past century. While tree growth slightly increased at the site closer to the Arctic Ocean, it declined after ca. 1950 at the more interior site. During the same period, tree-ring $\Delta^{13}C$ of white spruce and the inferred $_{i}WUE$ at both sites share the same increasing trajectories. Over the past century, we

found a slight but significant increase in $\Delta^{13}C$, and since ca. 1970, a continuous increase in $_{i}$WUE. Our results agree with the Brownlee et al. (2016) study in Alaska and suggest that drought-induced stomatal closure following the rise of temperature is unlikely the cause of the divergent white spruce growth trends found at our Arctic treeline sites.

Our study indicates that temperature and its interaction with other environmental variables such as sea ice extent and cloud cover have altered physiology and growth of treeline white spruce trees by influencing their photosynthetic assimilation, stomatal conductance, and growth rates over the last century. These physiological adjustments to environmental changes varied over the 20th century and caused loss or change in signs of correlations between the tree-ring isotopic ratios and climatic variables—the so called isotopic divergence (Savard & Daux, 2020). Overall, our findings indicate complex responses of treeline trees to changes in temperature, c_a, and sea ice extent at two remote locations. Lastly, our study highlights the need for further long-term and detailed studies across the Arctic on growth and physiological responses of trees to the rapid ongoing environmental changes. Such studies should comprise a gradient of permafrost conditions and include detailed soil temperature and moisture information to fully understand the influence of permafrost thaw and active layer thickness on trees' responses.

Conflict of Interest

The authors declare no conflicts of interest relevant to this study.

Data Availability Statement

Tree-ring width and stable carbon and oxygen isotope data supporting the conclusions of this study are available at the Arctic Data Center. For Coppermine, the tree-ring width chronology (D'Arrigo, Buckley, et al., 2023; https://doi.org/10.18739/A2QJ78043), carbon isotope discrimination (Andreu-Hayles et al., 2023a; https://doi.org/10.18739/A2G44HS0X) and stable oxygen isotope (Andreu-Hayles et al., 2023c; https://doi.org/10.18739/A26M3352T) records. For Thelon, the tree-ring width chronologies (D'Arrigo, Oelkers, et al., 2023; https://doi.org/10.18739/A2KS6J60Z), carbon isotope discrimination (Andreu-Hayles et al., 2023b; https://doi.org/10.18739/A2BC3SZ65) and stable oxygen isotope (Andreu-Hayles et al., 2023d; https://doi.org/10.18739/A22V2CB82) records.

Acknowledgments
This research was made possible through funding from NSF Grants PLR-1504134, OISE-1743738, and OPP-2124885. Rosanne D'Arrigo gratefully acknowledges the following NSF awards: Arctic Social Science GGO16659 and Arctic Natural Science NSF-2124885. The authors thank Wei Huang for the help with the isotopic analysis, the two reviewers for their constructive comments that helped to improve the manuscript, and Ben Gaglioti for the conversation about sea ice decline. Open access funding provided by Eidgenossische Technische Hochschule Zurich.

References

Andreu-Hayles, L., D'Arrigo, R., Anchukaitis, K. J., Beck, P. S. A., Frank, D., & Goetz, S. J. (2011a). Varying boreal forest response to Arctic environmental change at the Firth River, Alaska. *Environmental Research Letters*, *6*(4), 045503. https://doi.org/10.1088/1748-9326/6/4/045503

Andreu-Hayles, L., Gaglioti, B. V., Berner, L. T., Levesque, M., Anchukaitis, K. J., Goetz, S. J., & D'Arrigo, R. (2020). A narrow window of summer temperatures associated with shrub growth in Arctic Alaska. *Environmental Research Letters*, *15*(10), 105012. https://doi.org/10.1088/1748-9326/ab897f

Andreu-Hayles, L., Lévesque, M., Guerrieri, R., Siegwolf, R. T. W., & Körner, C. (2022). Limits and strengths of tree-ring stable isotopes. In R. T. W. Siegwolf, J. R. Brooks, J. Roden, & M. Saurer (Eds.), *Stable isotopes in tree rings: Inferring physiological, climatic and environmental responses* (pp. 399–428). Springer International Publishing. https://doi.org/10.1007/978-3-030-92698-4_14

Andreu-Hayles, L., Levesque, M., Martin-Benito, D., Huang, W., Harris, R., Oelkers, R., et al. (2019). A high-yield cellulose extraction system for small whole wood samples and dual measurement of carbon and oxygen stable isotopes. *Chemical Geology*, *504*, 53–65. https://doi.org/10.1016/j.chemgeo.2018.09.007

Andreu-Hayles, L., Oelkers, R., & Levesque, M. (2023a). Stable carbon isotope tree-ring records (Coppermine River, Nunavut, Canada) 1900–2003 [Dataset]. Arctic Data Center. https://doi.org/10.18739/A2G44HS0X

Andreu-Hayles, L., Oelkers, R., & Levesque, M. (2023b). Stable carbon isotope tree-ring records (Thelon River, Northwest Territories, Canada) 1900–2003 [Dataset]. Arctic Data Center. https://doi.org/10.18739/A2BC3SZ65

Andreu-Hayles, L., Oelkers, R., & Levesque, M. (2023c). Stable oxygen isotope tree-ring records (Coppermine River, Nunavut, Canada) 1900–2003 [Dataset]. Arctic Data Center. https://doi.org/10.18739/A26M3352T

Andreu-Hayles, L., Oelkers, R., & Levesque, M. (2023d). Stable oxygen isotope tree-ring records (Thelon River, Northwest Territories, Canada) 1900–2003 [Dataset]. Arctic Data Center. https://doi.org/10.18739/A22V2CB82

Andreu-Hayles, L., Planells, O., Gutiérrez, E., Muntan, E., Helle, G., Anchukaitis, K. J., & Schleser, G. H. (2011b). Long tree-ring chronologies reveal 20th century increases in water-use efficiency but no enhancement of tree growth at five Iberian pine forests. *Global Change Biology*, *17*(6), 2095–2112. https://doi.org/10.1111/j.1365-2486.2010.02373.x

Barber, V. A., Juday, G. P., & Finney, B. P. (2000). Reduced growth of Alaskan white spruce in the twentieth century from temperature-induced drought stress. *Nature*, *405*(6787), 668–673. https://doi.org/10.1038/35015049

Beaulne, J., Boucher, É., Garneau, M., & Magnan, G. (2021). Paludification reduces black spruce growth rate but does not alter tree water use efficiency in Canadian boreal forested peatlands. *Forest Ecosystems*, *8*(1), 28. https://doi.org/10.1186/s40663-021-00307-x

Beck, P. S. A., Juday, G. P., Alix, C., Barber, V. A., Winslow, S. E., Sousa, E. E., et al. (2011). Changes in forest productivity across Alaska consistent with biome shift. *Ecology Letters*, *14*(4), 373–379. https://doi.org/10.1111/j.1461-0248.2011.01598.x

Becker, A., Finger, P., Meyer-Christoffer, A., Rudolf, B., Schamm, K., Schneider, U., & Ziese, M. (2013). A description of the global land-surface precipitation data products of the Global Precipitation Climatology Centre with sample applications including centennial (trend) analysis from 1901 to present. *Earth System Science Data*, *5*(1), 71–99. https://doi.org/10.5194/essd-5-71-2013

Berner, L. T., Massey, R., Jantz, P., Forbes, B. C., Macias-Fauria, M., Myers-Smith, I., et al. (2020). Summer warming explains widespread but not uniform greening in the Arctic tundra biome. *Nature Communications*, *11*(1), 4621. https://doi.org/10.1038/s41467-020-18479-5

Bradshaw, C. J. A., & Warkentin, I. G. (2015). Global estimates of boreal forest carbon stocks and flux. *Global and Planetary Change*, *128*, 24–30. https://doi.org/10.1016/j.gloplacha.2015.02.004

Brennan, M. K., Hakim, G. J., & Blanchard-Wrigglesworth, E. (2020). Arctic sea-ice variability during the instrumental era. *Geophysical Research Letters*, *47*(7), e2019GL086843. https://doi.org/10.1029/2019GL086843

Bronaugh, D., & Werner, A. (2019). *zyp: Zhang + Yue-Pilon trends package., R package version 0.10-1.1*. R Foundation for Statistical Computing.

Brownlee, A. H., Sullivan, P. F., Csank, A. Z., Sveinbjörnsson, B., & Ellison, S. B. Z. (2016). Drought-induced stomatal closure probably cannot explain divergent white spruce growth in the Brooks Range, Alaska, USA. *Ecology*, *97*(1), 145–159. https://doi.org/10.1890/15-0338.1

Buchwal, A., Sullivan, P. F., Macias-Fauria, M., Post, E., Myers-Smith, I. H., Stroeve, J. C., et al. (2020). Divergence of Arctic shrub growth associated with sea ice decline. *Proceedings of the National Academy of Sciences*, *117*(52), 33334–33344. https://doi.org/10.1073/pnas.2013311117

Budikova, D. (2009). Role of Arctic sea ice in global atmospheric circulation: A review. *Global and Planetary Change*, *68*(3), 149–163. https://doi.org/10.1016/j.gloplacha.2009.04.001

Cabon, A., Kannenberg, S. A., Arain, A., Babst, F., Baldocchi, D., Belmecheri, S., et al. (2022). Cross-biome synthesis of source versus sink limits to tree growth. *Science*, *376*(6594), 758–761. https://doi.org/10.1126/science.abm4875

Cai, Q., Wang, J., Beletsky, D., Overland, J., Ikeda, M., & Wan, L. (2021). Accelerated decline of summer Arctic sea ice during 1850–2017 and the amplified Arctic warming during the recent decades. *Environmental Research Letters*, *16*(3), 034015. https://doi.org/10.1088/1748-9326/abdb5f

Cernusak, L. A., Haverd, V., Brendel, O., Le Thiec, D., Guehl, J.-M., & Cuntz, M. (2019). Robust response of terrestrial plants to rising CO_2. *Trends in Plant Science*, *24*(7), 578–586. https://doi.org/10.1016/j.tplants.2019.04.003

Chapin, F. S., McGuire, A., Ruess, R., Hollingsworth, T., Mack, M., Johnstone, J., et al. (2010). Resilience of Alaska's boreal forest to climatic change. *Canadian Journal of Forest Research*, *40*(7), 1360–1370. https://doi.org/10.1139/x10-074

Chapin, F. S., Sturm, M., Serreze, M. C., McFadden, J. P., Key, J. R., Lloyd, A. H., et al. (2005). Role of land-surface changes in Arctic summer warming. *Science*, *310*(5748), 657–660. https://doi.org/10.1126/science.1117368

Dansgaard, W. (1964). Stable isotopes in precipitation. *Tellus*, *16*(4), 436–468. https://doi.org/10.1111/j.2153-3490.1964.tb00181.x

D'Arrigo, R., Buckley, B., Oelkers, R., Levesque, M., & Andreu-Hayles, L. (2023). Tree-ring width series of white spruce (*Picea glauca*) trees (Coppermine River, Canada) 1676-2003 [Dataset]. Arctic Data Center. https://doi.org/10.18739/A2QJ78043

D'Arrigo, R., Jacoby, G., Buckley, B., Sakulich, J., Frank, D., Wilson, R., et al. (2009). Tree growth and inferred temperature variability at the North American Arctic treeline. *Global and Planetary Change*, *65*(1), 71–82. https://doi.org/10.1016/j.gloplacha.2008.10.011

D'Arrigo, R., Oelkers, R., Levesque, M., & Andreu-Hayles, L. (2023). Tree-ring width series of white spruce (*Picea glauca*) trees (Thelon River Canada) 1661–2003 [Dataset]. Arctic Data Center. https://doi.org/10.18739/A2KS6J60Z

D'Arrigo, R., Wilson, R., & Jacoby, G. (2006). On the long-term context for late 20th-century warming. *Journal of Geophysical Research: Atmospheres*, *111*(D3), D03103. https://doi.org/10.1029/2005JD006352

D'Arrigo, R., Wilson, R., Liepert, B., & Cherubini, P. (2008). On the "divergence problem" in northern forests: A review of the tree-ring evidence and possible causes. *Global and Planetary Change*, *60*(3), 289–305. https://doi.org/10.1016/j.gloplacha.2007.03.004

Faber, A. K., Møllesøe Vinther, B., Sjolte, J., & Anker Pedersen, R. (2017). How does sea ice influence $\delta^{18}O$ of Arctic precipitation? *Atmospheric Chemistry and Physics*, *17*(9), 5865–5876. https://doi.org/10.5194/acp-17-5865-2017

Farquhar, G., O'Leary, M., & Berry, J. (1982). On the relationship between carbon isotope discrimination and the intercellular carbon dioxide concentration in leaves. *Australian Journal of Plant Physiology*, *9*(2), 121. https://doi.org/10.1071/PP9820121

Farquhar, G., & Richards, R. (1984). Isotopic composition of plant carbon correlates with water-use efficiency of wheat genotypes. *Australian Journal of Plant Physiology*, *11*(6), 539–552. https://doi.org/10.1071/PP9840539

Field, R. D., Andreu-Hayles, L., D'arrigo, R. D., Oelkers, R., Luckman, B. H., Morimoto, D., et al. (2022). Tree-ring cellulose $\delta^{18}O$ records similar large-scale climate influences as precipitation $\delta^{18}O$ in the Northwest Territories of Canada. *Climate Dynamics*, *58*(3), 759–776. https://doi.org/10.1007/s00382-021-05932-4

Gaglioti, B. V., Mann, D. H., Wooller, M. J., Jones, B. M., Wiles, G. C., Groves, P., et al. (2017). Younger-Dryas cooling and sea-ice feedbacks were prominent features of the Pleistocene-Holocene transition in Arctic Alaska. *Quaternary Science Reviews*, *169*, 330–343. https://doi.org/10.1016/j.quascirev.2017.05.012

Girardin, M. P., Bouriaud, O., Hogg, E. H., Kurz, W., Zimmermann, N. E., Metsaranta, J. M., et al. (2016). No growth stimulation of Canada's boreal forest under half-century of combined warming and CO_2 fertilization. *Proceedings of the National Academy of Sciences*, *113*(52), E8406–E8414. https://doi.org/10.1073/pnas.1610156113

Girardin, M. P., Guo, X. J., De Jong, R., Kinnard, C., Bernier, P., & Raulier, F. (2014). Unusual forest growth decline in boreal North America covaries with the retreat of Arctic sea ice. *Global Change Biology*, *20*(3), 851–866. https://doi.org/10.1111/gcb.12400

Grossiord, C., Buckley, T. N., Cernusak, L. A., Novick, K. A., Poulter, B., Siegwolf, R. T. W., et al. (2020). Plant responses to rising vapor pressure deficit. *New Phytologist*, *226*(6), 1550–1566. https://doi.org/10.1111/nph.16485

Harris, I., Osborn, T. J., Jones, P., & Lister, D. (2020). Version 4 of the CRU TS monthly high-resolution gridded multivariate climate data set. *Scientific Data*, *7*(1), 109. https://doi.org/10.1038/s41597-020-0453-3

Hegerl, G. C., Brönnimann, S., Schurer, A., & Cowan, T. (2018). The early 20th century warming: Anomalies, causes, and consequences. *WIREs Climate Change*, *9*(4), e522. https://doi.org/10.1002/wcc.522

Jacoby, G. C., & D'Arrigo, R. D. (1995). Tree ring width and density evidence of climatic and potential forest change in Alaska. *Global Biogeochemical Cycles*, *9*(2), 227–234. https://doi.org/10.1029/95GB00321

Jones, A., Stolbovoy, V., Tarnocai, C., Broll, G., Spaargaren, O., & Montanarella, L. e. (2009). *Soil Atlas of the northern circumpolar region* (p. 142). European Commission, Office for Official Publications of the European Communities.

Kaufman, D. S., Schneider, D. P., McKay, N. P., Ammann, C. M., Bradley, R. S., Briffa, K. R., et al. (2009). Recent warming reverses long-term Arctic cooling. *Science*, *325*(5945), 1236–1239. https://doi.org/10.1126/science.1173983

Kopec, B. G., Feng, X., Michel, F. A., & Posmentier, E. S. (2016). Influence of sea ice on Arctic precipitation. *Proceedings of the National Academy of Sciences*, *113*(1), 46–51. https://doi.org/10.1073/pnas.1504633113

Körner, C. (2012). *Alpine treelines: Functional ecology of the global high elevation tree limits* (p. 220). Springer. https://doi.org/10.1007/978-3-0348-0396-0

Lavergne, A., Graven, H., De Kauwe, M. G., Keenan, T. F., Medlyn, B. E., & Prentice, I. C. (2019). Observed and modeled historical trends in the water-use efficiency of plants and ecosystems. *Global Change Biology*, *25*(7), 2242–2257. https://doi.org/10.1111/gcb.14634

Lefcheck, J. S. (2016). piecewiseSEM: Piecewise structural equation modeling in R for ecology, evolution, and systematics. *Methods in Ecology and Evolution*, *7*(5), 573–579. https://doi.org/10.1111/2041-210X.12512

Lévesque, M., Siegwolf, R., Saurer, M., Eilmann, B., & Rigling, A. (2014). Increased water-use efficiency does not lead to enhanced tree growth under xeric and mesic conditions. *New Phytologist*, *203*(1), 94–109. https://doi.org/10.1111/nph.12772

Little, E. L., Jr. (1971). *Atlas of United States trees. Volume 1. Conifers and important hardwoods* (p. 9). Forest Service.

Lloyd, A. H., & Bunn, A. G. (2007). Responses of the circumpolar boreal forest to 20th century climate variability. *Environmental Research Letters*, *2*(4), 045013. https://doi.org/10.1088/1748-9326/2/4/045013

Lloyd, A. H., & Fastie, C. L. (2002). Spatial and temporal variability in the growth and climate response of treeline trees in Alaska. *Climatic Change*, *52*(4), 481–509. https://doi.org/10.1023/A:1014278819094

McCarroll, D., & Loader, N. J. (2004). Stable isotopes in tree rings. *Quaternary Science Reviews*, *23*(7–8), 771–801. https://doi.org/10.1016/j.quascirev.2003.06.017

McGuire, A. D., Anderson, L. G., Christensen, T. R., Dallimore, S., Guo, L., Hayes, D. J., et al. (2009). Sensitivity of the carbon cycle in the Arctic to climate change. *Ecological Monographs*, *79*(4), 523–555. https://doi.org/10.1890/08-2025.1

McGuire, A. D., Ruess, R. W., Lloyd, A. H., Yarie, J., Clein, J. S., & Juday, G. P. (2010). Vulnerability of white spruce tree growth in interior Alaska in response to climate variability: Dendrochronological, demographic, and experimental perspectives. *Canadian Journal of Forest Research*, *40*(7), 1197–1209. https://doi.org/10.1139/X09-206

Mellat, M., Bailey, H., Mustonen, K. R., Marttila, H., Klein, E. S., Gribanov, K., et al. (2021). Hydroclimatic controls on the isotopic (δ^{18} O, δ^{2} H, *d-excess*) traits of pan-Arctic summer rainfall events. *Frontiers of Earth Science*, *9*. https://doi.org/10.3389/feart.2021.651731

Nicklen, E. F., Roland, C. A., Csank, A. Z., Wilmking, M., Ruess, R. W., & Muldoon, L. A. (2019). Stand basal area and solar radiation amplify white spruce climate sensitivity in interior Alaska: Evidence from carbon isotopes and tree rings. *Global Change Biology*, *25*(3), 911–926. https://doi.org/10.1111/gcb.14511

Nicklen, E. F., Roland, C. A., Ruess, R. W., Scharnweber, T., & Wilmking, M. (2021). Divergent responses to permafrost and precipitation reveal mechanisms for the spatial variation of two sympatric spruce. *Ecosphere*, *12*(7), e03622. https://doi.org/10.1002/ecs2.3622

Norby, R. J., Warren, J. M., Iversen, C. M., Medlyn, B. E., & McMurtrie, R. E. (2010). CO_2 enhancement of forest productivity constrained by limited nitrogen availability. *Proceedings of the National Academy of Sciences*, *107*(45), 19368–19373. https://doi.org/10.1073/pnas.1006463107

O'Leary, M. H. (1981). Carbon isotope fractionation in plants. *Phytochemistry*, *20*(4), 553–567. https://doi.org/10.1016/0031-9422(81)85134-5

Pan, Y., Birdsey, R. A., Fang, J., Houghton, R., Kauppi, P. E., Kurz, W. A., et al. (2011). A large and persistent carbon sink in the world's forests. *Science*, *333*(6045), 988–993. https://doi.org/10.1126/science.1201609

Patankar, R., Quinton, W. L., Hayashi, M., & Baltzer, J. L. (2015). Sap flow responses to seasonal thaw and permafrost degradation in a subarctic boreal peatland. *Trees*, *29*(1), 129–142. https://doi.org/10.1007/s00468-014-1097-8

Pearson, R. G., Phillips, S. J., Loranty, M. M., Beck, P. S. A., Damoulas, T., Knight, S. J., & Goetz, S. J. (2013). Shifts in Arctic vegetation and associated feedbacks under climate change. *Nature Climate Change*, *3*(7), 673–677. https://doi.org/10.1038/nclimate1858

Peñuelas, J., Canadell, J. G., & Ogaya, R. (2011). Increased water-use efficiency during the 20th century did not translate into enhanced tree growth. *Global Ecology and Biogeography*, *20*(4), 597–608. https://doi.org/10.1111/j.1466-8238.2010.00608.x

Peters, R. L., Groenendijk, P., Vlam, M., & Zuidema, P. A. (2015). Detecting long-term growth trends using tree rings: A critical evaluation of methods. *Global Change Biology*, *21*(5), 2040–2054. https://doi.org/10.1111/gcb.12826

Pinheiro, J., Bates, D., DebRoy, S., & Sarkar, D. (2013). Linear and nonlinear mixed effects models. *nlme* R package version 3 (pp. 1–113).

Pisaric, M., Carey, S., Kokelj, S., & Youngblut, D. (2007). Anomalous 20th century tree growth, Mackenzie Delta, Northwest Territories, Canada. *Geophysical Research Letters*, *34*(5), L05714. https://doi.org/10.1029/2006GL029139

Porter, T. J., & Pisaric, M. F. J. (2011). Temperature-growth divergence in white spruce forests of Old Crow Flats, Yukon Territory, and adjacent regions of northwestern North America. *Global Change Biology*, *17*(11), 3418–3430. https://doi.org/10.1111/j.1365-2486.2011.02507.x

Post, E., Bhatt, U. S., Bitz, C. M., Brodie, J. F., Fulton, T. L., Hebblewhite, M., et al. (2013). Ecological consequences of sea-ice decline. *Science*, *341*(6145), 519–524. https://doi.org/10.1126/science.1235225

Rossi, S., Anfodillo, T., Čufar, K., Cuny, H. E., Deslauriers, A., Fonti, P., et al. (2013). A meta-analysis of cambium phenology and growth: Linear and nonlinear patterns in conifers of the northern hemisphere. *Annals of Botany*, *112*(9), 1911–1920. https://doi.org/10.1093/aob/mct243

Saurer, M., Kirdyanov, A. V., Prokushkin, A. S., Rinne, K. T., & Siegwolf, R. T. W. (2016). The impact of an inverse climate-isotope relationship in soil water on the oxygen-isotope composition of *Larix gmelinii* in Siberia. *New Phytologist*, *209*(3), 955–964. https://doi.org/10.1111/nph.13759

Saurer, M., Schweingruber, F., Vaganov, E. A., Shiyatov, S. G., & Siegwolf, R. (2002). Spatial and temporal oxygen isotope trends at the northern tree-line in Eurasia. *Geophysical Research Letters*, *29*(9), 7-1–7-4. https://doi.org/10.1029/2001GL013739

Saurer, M., Siegwolf, R. T. W., & Schweingruber, F. H. (2004). Carbon isotope discrimination indicates improving water-use efficiency of trees in northern Eurasia over the last 100 yr. *Global Change Biology*, *10*(12), 2109–2120. https://doi.org/10.1111/j.1365-2486.2004.00869.x

Saurer, M., Spahni, R., Frank, D. C., Joos, F., Leuenberger, M., Loader, N. J., et al. (2014). Spatial variability and temporal trends in water-use efficiency of European forests. *Global Change Biology*, *20*(12), 3700–3712. https://doi.org/10.1111/gcb.12717

Savard, M. M., & Daux, V. (2020). An overview on isotopic divergences—Causes for instability of tree-ring isotopes and climate correlations. *Climate of the Past*, *16*(4), 1223–1243. https://doi.org/10.5194/cp-16-1223-2020

Schneider, U., Becker, A., Finger, P., Meyer-Christoffer, A., & Ziese, M. (2018). GPCC full data monthly product version 2018 at 0.25°: Monthly land-surface precipitation from rain-gauges built on GTS-based and historical data, https://doi.org/10.5676/DWD_GPCC/FD_M_V2018_025

Seddon, A. W. R., Macias-Fauria, M., Long, P. R., Benz, D., & Willis, K. J. (2016). Sensitivity of global terrestrial ecosystems to climate variability. *Nature*, *531*(7593), 229–232. https://doi.org/10.1038/nature16986

Seibt, U., Rajabi, A., Griffiths, H., & Berry, J. (2008). Carbon isotopes and water use efficiency: Sense and sensitivity. *Oecologia*, *155*(3), 441–454. https://doi.org/10.1007/s00442-007-0932-7

Serreze, M. C., Holland, M. M., & Stroeve, J. (2007). Perspectives on the Arctic's shrinking sea-ice cover. *Science*, *315*(5818), 1533–1536. https://doi.org/10.1126/science.1139426

Smith, S. L., O'Neill, H. B., Isaksen, K., Noetzli, J., & Romanovsky, V. E. (2022). The changing thermal state of permafrost. *Nature Reviews Earth & Environment*, *3*(1), 10–23. https://doi.org/10.1038/s43017-021-00240-1

Sniderhan, A. E., & Baltzer, J. L. (2016). Growth dynamics of black spruce (*Picea mariana*) in a rapidly thawing discontinuous permafrost peatland. *Journal of Geophysical Research: Biogeosciences*, *121*(12), 2988–3000. https://doi.org/10.1002/2016JG003528

Sniderhan, A. E., Mamet, S. D., & Baltzer, J. L. (2021). Non-uniform growth dynamics of a dominant boreal tree species (*Picea mariana*) in the face of rapid climate change. *Canadian Journal of Forest Research*, *51*(4), 565–572. https://doi.org/10.1139/cjfr-2020-0188

Sugimoto, A. (2019). Stable isotopes of water in permafrost ecosystem. In T. Ohta, T. Hiyama, Y. Iijima, A. Kotani, & T. C. Maximov (Eds.), *Water-carbon dynamics in Eastern Siberia* (pp. 135–151). Springer. https://doi.org/10.1007/978-981-13-6317-7_6

Sullivan, P. F., Pattison, R. R., Brownlee, A. H., Cahoon, S. M. P., & Hollingsworth, T. N. (2016). Effect of tree-ring detrending method on apparent growth trends of black and white spruce in interior Alaska. *Environmental Research Letters*, *11*(11), 114007. https://doi.org/10.1088/1748-9326/11/11/114007

Sullivan, P. F., Pattison, R. R., Brownlee, A. H., Cahoon, S. M. P., & Hollingsworth, T. N. (2017). Limited evidence of declining growth among moisture-limited black and white spruce in interior Alaska. *Scientific Reports*, *7*(1), 15344. https://doi.org/10.1038/s41598-017-15644-7

Sun, Q., Miao, C., Duan, Q., Ashouri, H., Sorooshian, S., & Hsu, K.-L. (2018). A review of global precipitation data sets: Data sources, estimation, and intercomparisons. *Reviews of Geophysics*, *56*(1), 79–107. https://doi.org/10.1002/2017RG000574

Vihma, T. (2014). Effects of Arctic sea ice decline on weather and climate: A review. *Surveys in Geophysics*, *35*(5), 1175–1214. https://doi.org/10.1007/s10712-014-9284-0

Visser, H. (1995). Note on the relation between ring widths and basal area increments. *Forest Science*, *41*(2), 297–304. https://doi.org/10.1093/forestscience/41.2.297

Voltas, J., Aguilera, M., Gutiérrez, E., & Shestakova, T. A. (2020). Shared drought responses among conifer species in the middle Siberian taiga are uncoupled from their contrasting water-use efficiency trajectories. *Science of the Total Environment*, *720*, 137590. https://doi.org/10.1016/j.scitotenv.2020.137590

Walker, X. J., Mack, M. C., & Johnstone, J. F. (2015). Stable carbon isotope analysis reveals widespread drought stress in boreal black spruce forests. *Global Change Biology*, *21*(8), 3102–3113. https://doi.org/10.1111/gcb.12893

Walsh, J. E., Chapman, W. L., Fetterer, F., & Stewart, J. S. (2019). *Gridded monthly sea ice extent and concentration, 1850 onward, Version 2*. NSIDC: National Snow and Ice Data Center. https://doi.org/10.7265/jj4s-tq79

Walsh, J. E., Fetterer, F., Scott Stewart, J., & Chapman, W. L. (2017). A database for depicting Arctic sea ice variations back to 1850. *Geographical Review*, *107*(1), 89–107. https://doi.org/10.1111/j.1931-0846.2016.12195.x

Wigley, T. M. L., Briffa, K. R., & Jones, P. D. (1984). On the average value of correlated time series, with applications in dendroclimatology and hydrometeorology. *Journal of Applied Meteorology and Climatology*, *23*(2), 201–213. https://doi.org/10.1175/1520-0450(1984)023<0201:OTAVOC>2.0.CO;2

Wilmking, M., Juday, G. P., Barber, V. A., & Zald, H. S. J. (2004). Recent climate warming forces contrasting growth responses of white spruce at treeline in Alaska through temperature thresholds. *Global Change Biology*, *10*(10), 1724–1736. https://doi.org/10.1111/j.1365-2486.2004.00826.x

Yamanouchi, T. (2011). Early 20th century warming in the Arctic: A review. *Polar Science*, *5*(1), 53–71. https://doi.org/10.1016/j.polar.2010.10.002

Yue, S., Pilon, P., Phinney, B., & Cavadias, G. (2002). The influence of autocorrelation on the ability to detect trend in hydrological series. *Hydrological Processes*, *16*(9), 1807–1829. https://doi.org/10.1002/hyp.1095

Zang, C., & Biondi, F. (2015). treeclim: An R package for the numerical calibration of proxy-climate relationships. *Ecography*, *38*(4), 431–436. https://doi.org/10.1111/ecog.01335

Zuur, A. F., Ieno, E. N., Walker, N., Saveliev, A. A., & Smith, G. M. (2009). *Mixed effects models and extensions in ecology with R*. Springer. https://doi.org/10.1007/978-0-387-87458-6